Journal of Materials Chemistry B

ROYAL SOCIETY OF CHEMISTRY

REVIEW

View Article Online
View Journal | View Issue

Cite this: J. Mater. Chem. B, 2023, 11, 6782

Metal–organic frameworks (MOFs) as effectual diagnostic and therapeutic tools for cancer

Shikha Gulati, *[a] Akangkha Choudhury,[b] Gauravya Mohan,[b] Riya Katiyar,[a] Mohammed Abaan Kurikkal M P,[b] Sanjay Kumar*[a] and Rajender S. Varma *[c]

Received 31st March 2023,
Accepted 5th June 2023

DOI: 10.1039/d3tb00706e

rsc.li/materials-b

Metal–organic frameworks (MOFs) are a class of multifunctional organometallic compounds that include metal ions combined with assorted organic linkers. Recently, these compounds have received widespread attention in medicine, due to their exceptional qualities, including a wide surface area, high porosity, outstanding biocompatibility, non-toxicity, *etc.* Such characteristic qualities make MOFs superb candidates for biosensing, molecular imaging, drug delivery, and enhanced cancer therapies. This review illustrates the key attributes of MOFs and their importance in cancer research. The structural and synthetic aspects of MOFs are briefly discussed with primary emphasis on diagnostic and therapeutic features, as well as their performance and significance in modern therapeutic methods and synergistic theranostic strategies including biocompatibility. This review offers cumulative scrutiny of the widespread appeal of MOFs in modern-day oncological research, which may stimulate further explorations.

1. Introduction

Today, cancer stands among the most dreadful diseases in the world. It accounts for more than 10 million deaths each year or one in every six deaths, and has become a multifaceted global health challenge that demands action.[1] Conventional cancer treatments involve processes such as radiation, chemotherapy, and surgery. But, poor specificity, heavy dependence on higher drug concentrations, poor bioavailability, immunosuppression, strong side effects, and the inability to cope with drug-resistant variants have rendered these strategies ineffective as a permanent cure for cancer. The drawbacks in the traditional treatments have led the way for modern oncological research to develop novel techniques which can deliver highly effective results in the diagnosis of cancer and therapeutic treatments.

Metal–organic frameworks (MOFs), also called porous coordination polymers (PCPs), are excellent nanoplatforms that have shown promising potential in numerous anti-cancer studies. They are a special category of hybrid, crystalline coordination compounds consisting of metal ions and organic linkers, and have lately garnered immense interest for use in catalysis, separation, and biological applications. Compared to other nanoparticles, MOFs are endowed with a plethora of advantages. Due to their extremely versatile nature, a variety of metal ions and organic linkers can be combined based on their physical and chemical differences and target functions.[2] This dynamic flexibility is well exploited not just in biomedical research, but also for addressing environmental threats and attaining a sustainable solution to our needs; MOFs serve as excellent adsorbents for adsorptive desulfurization of fossil fuels.[3]

Diversely functionalized nanoparticles and functional groups can be incorporated into MOFs *via* surface modifications and post-synthetic routes to tailor multifunctional nanocomposites that can be deployed for a wide array of purposes. The ability to modify such materials enables the preparation of a myriad of MOFs. Every MOF so composed exhibits its own characteristic physical and chemical features and thus can be employed as a unique vehicle for distinct treatment methods accordingly. The metal ions in these frameworks offer the possibility of magnetic stimulation and can serve as imaging contrast agents in various molecular imaging techniques like X-ray computed tomography (CT), photoacoustic imaging (PAI), magnetic resonance imaging (MRI), and fluorescence imaging (FI), amongst others. The high porosity and huge surface area of MOFs allow swift capture of biomarkers that can be subsequently detected through fluorescence. Due to their dual functions of imaging and biosensing, MOFs have exhibited remarkable success in cancer diagnosis.[4–6]

The huge surface area, high porosity, and large size of pores in MOFs contribute to great drug-loading capacity, making them ideal carriers in drug delivery. Further, since these materials are linked by weak coordination bonds, they are biodegradable and easy to metabolize. Effective medication distribution is critical for

[a] Department of Chemistry, Sri Venkateswara College, University of Delhi, Delhi 110021, India. E-mail: shikha2gulati@gmail.com, kumarsanjaybatra20@gmail.com
[b] Department of Biological Sciences, Sri Venkateswara College, University of Delhi, Delhi 110021, India
[c] Centre of Excellence for Research in Sustainable Chemistry, Department of Chemistry, Federal University of São Carlos, 13565 905 São Carlos – SP, Brazil. E-mail: rajvarma@hotmail.com

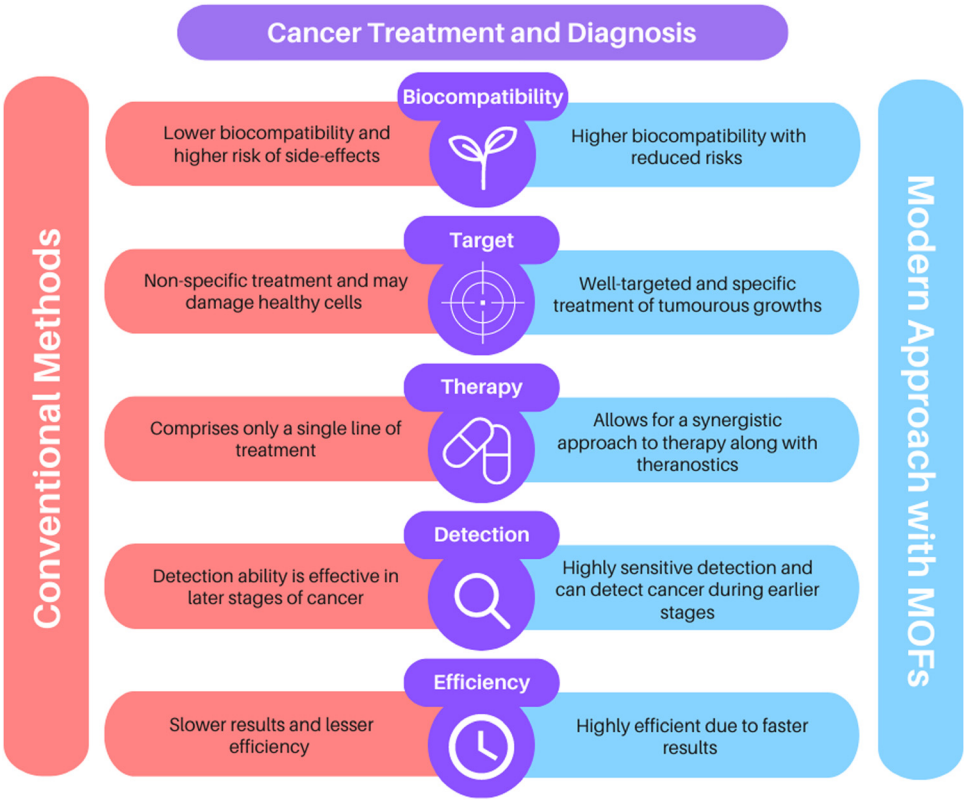

Fig. 1 Benefits of the MOF-based approach for cancer therapy over conventional methods.

treating diseases and is still a major obstacle in medicine. Chemotherapeutic drugs lack the ability to distinguish between healthy cells and cancer cells, and thus they damage the normal cells too in the process of treatment, leading to numerous undesired side effects. Recent developments in the field of microfabrication have made it possible to create controlled-release medication delivery devices (Fig. 1). Several MOFs can serve as well-targeted drug delivery systems based on stimuli-responsive microenvironments like pH, magnetic fields, and temperature. Furthermore, specialized nanoscale metal–organic frameworks (NMOFs) serve as photosensitizers (PSs) in photo-therapies like photothermal therapy (PTT) and photodynamic therapy (PDT).[7,8]

Recent developments in the field of microfabrication have made it possible to create controlled-release medication delivery devices, and biomedical applications of nanomaterials and herein, the important biomedical applications of MOFs in the treatment of cancer are mainly focussed (Fig. 2).[4–8] While most

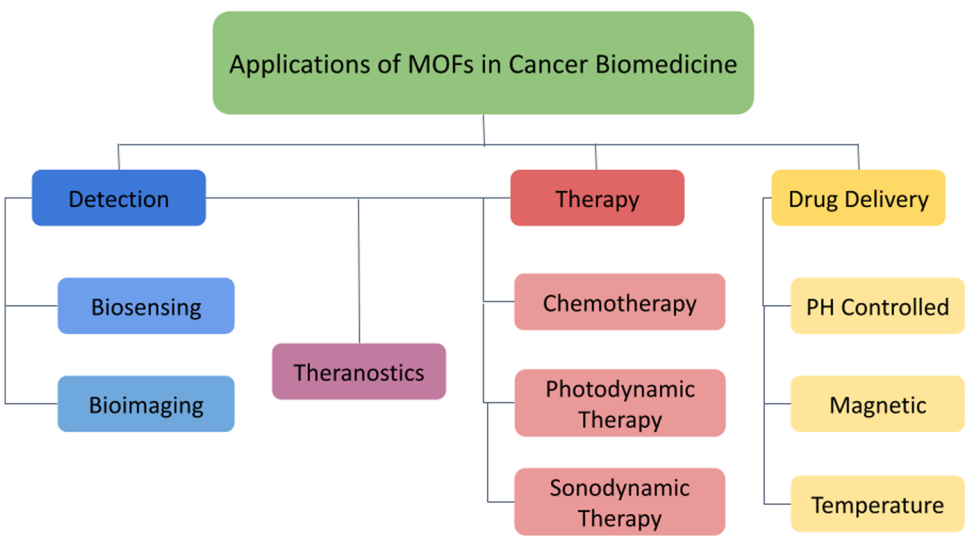

Fig. 2 Applications of MOFs in cancer biomedicine.

of the existing reviews only offer centralized information about a single stratum of application,[9–12] we have provided a multifaceted-multidimensional review that has holistically discussed the structure and synthesis of MOFs, the role of MOFs in cancer detection and drug delivery, including modern therapeutic strategies such as photothermal therapy, starvation therapy, photodynamic therapy, sonodynamic therapy, as well as synergistic approaches like combination therapies and multimodal theranostics.

An excellent review written by Yang *et al.* focuses more on the functionalization of MOFs in biomedicine, rather than targeting the mechanisms for inhibiting cancer.[13] Our review is unique in this regard as it specializes exclusively in cancer biomedicine, as opposed to covering all other biomedical applications of MOFs. The mechanistic aspects are well described leading to tumor suppression through various therapies with relevant discussion on their respective principles of working. Similarly, the reviews by Wu *et al.* and Wang *et al.* showcase MOFs as ideal nanoplatforms for cargo delivery and theranostics.[14,15] Specific details for the individual treatment procedures like photodynamic therapy (PDT), sonodynamic therapy (SDT), *etc.* have been missing. Our review takes clear account of the significant procedures in cancer treatment independently and elaborately in distinct sections, along with incorporating these techniques in theranostics and synergistic treatments. Further, we have also discussed biocompatibility and cytotoxicity issues for MOFs, which highlights them in a positive light as prospective candidates in the world of nanomedicine.

2. Structure and synthesis of MOFs

Metal–organic frameworks are created by the combination of metal ions (nodes), either single or mixed, with organic or bio-based ligands (linkers). These materials are highly versatile due to their mixed chemical nature. The high surface area due to their nanostructures allows for the modification and adsorption of substances. The myriad of options for metal nodes as well as linkers combined with numerous post-modifications has allowed a large number of MOFs to be developed.[16,17]

2.1 Methods for synthesis

Conditions of the reaction such as the temperature can affect the morphological, physical, and chemical properties of MOFs[16,17] as they can be prepared across a range of temperatures which can influence their structures. The preparation can also be conducted at room temperature, elevated temperatures, or even under solvothermal conditions with the use of an autoclave; the synthesis methods include conventional heating as well as contemporary strategies such as electrochemical, mechanochemical, and sonochemical syntheses.

(i) Solvothermal/hydrothermal synthesis. The conventional methods of MOF preparation involve slow stirring of various reagents to produce nanoparticles. Pan *et al.*'s preparation of ZIF-8 by the addition of zinc nitrate solution to 2-methylimidazole is one such example that was carried out at room temperature.[18] A white cloudy precipitate was formed which was washed with deionized water (Table 1, entry 1). You-Kyong Seo *et al.* prepared the MOF iron(III) trimesate MIL-100(Fe) by the addition of trimesic acid to ferric nitrate solution.[19] The reaction mixture was subsequently heated to 160 °C. A light orange product was obtained and then purified through filtration and washing with deionized water (Table 1, entry 2).

The contemporary methods of MOF preparation require advanced techniques based on microwave, electrochemistry, mechanochemistry, and sonochemistry.

(ii) Sonochemical synthesis. This method involves the formation and collapse of a bubble within a liquid. This causes high localized pressures and temperatures. The result is homogeneous nucleation and a fall in crystallization time as compared to conventional methods. Won-Jin Son *et al.* prepared MOF5 from a mixture of zinc nitrate, terephthalic acid, and NMP using sonochemistry;[20] sonicators have been used to precipitate out white crystals of the MOF from the solution (Table 1, entry 3).

(iii) Mechanochemical synthesis. Mechanical energy is applied to reaction materials to prepare the products. This can be accomplished through a ball mill, and the addition of beads can increase the milling process. Jethro Beamish-Cook *et al.* prepared MOF-74 from zinc oxide and 2,5-dihydroxyterephthalic acid (H4DHTA) by mechanochemical synthesis.[21] The materials were placed inside a grinding jar with stainless-steel beads along with dimethylformamide (DMF) as a liquid additive. Milling was carried out at a rate of 40 Hz. A Retsch MM400 shaker-type mixer mill was used to obtain the MOF (Table 1, entry 4).

2.2 Structure and relative function

The primary factor affecting the structure of MOFs is the metal node and organic linker deployed in the preparation of MOFs

Table 1 Overview of synthesis methods for some MOFs commonly used in cancer medicine

Entry	MOF studied	Attributes studied	Findings	Ref.
1	ZIF-8	Conventional synthesis and structure	Preparation by simple precipitation. Cubic symmetry. Metal centres are tetrahedral and coordinated by nitrogen atoms	18, 22, 23, 39 and 42
2	MIL-100(Fe)	Conventional synthesis and structure	Preparation by heating and precipitation. Super tetrahedral structure.	19, 24–26 and 47
3	MOF-5(Zn)	Sonochemical synthesis	White crystals of the MOF were precipitated out of the solution *via* sonication. This reduced the time, yielded smaller crystals, and was more economic as compared to conventional methods	20
4	MOF-74(Zn)	Mechanochemical synthesis	Helical rods of the MOFs were prepared through milling. The solvent molecules were structurally integrated into the intermediate phases during the reaction. Hence, the solvent plays a major role in the final structure	21

which decide the symmetry of the final molecule. However, synthesis conditions (such as temperature and pressure)[14,15] affect the MOF structure as well. Though the similarity in symmetry is largely consistent, the structures may vary in pore size, pore distribution, or dimensional angles. Structural elements also impart specific properties to the final product. Surface modifications can be used to load drugs,[30] magnetic components[19] can be added and even complexes of various MOFs[23] can be created.

The structure is often visualized through X-ray diffraction techniques (Fig. 3). However, it must be noted that since the preparation of MOFs is rather expensive, studies on the structure are usually conducted with the help of molecular simulation approaches. MOFs are available in a plethora of shapes and sizes with two such MOFs being discussed hereafter.

The MOF ZIF-8 comprises 2-methylimidazolate (mIm) as a substituted imidazolate-type linker. The metal centres are tetrahedral. Coordination occurs at 1,3-positions of the imidazolate bridging ligand by nitrogen atoms. The substitution is responsible for cubic symmetry, relatively low densities, large surface areas, and high porosity. Hence, ZIF-8 is categorized as a low-density open framework. Nanoindentation studies of such frameworks through single-crystal X-ray diffraction reveal that they exhibit relatively low stiffness with their elastic modulus, the values of which are usually 3–4 GPa. The cubic structure is attributed to large surface accessible volume (SAV) and high porosity, a property that renders ZIF-8 MOFs extremely favorable for drug delivery and cancer detection purposes.[22] High porosity and surface area allow for the loading of drugs while low densities favour mobility. ZIF-8 has a pH-dependent structure which allows for the controlled release of drugs at required locations.[23]

The cubic symmetry of ZIF-8 allows it to have a highly porous framework. This increases the surface area of the material which allows for surface modification for drug loading[22] thus enabling a larger amount of the drug to be loaded. These modifications also allow for the controlled and specific release of the drug in tumorous cells, so as to avoid cytotoxicity in healthy cells, making this drug delivery highly biocompatible as compared to conventional methods.[22]

Fe-Based MOFs are another important class of MOFs in cancer research wherein diverse structures are possible based on the type of linkers and core cluster-building units. Most of these MOFs have Fe in the +3 oxidation state and use carboxylate-based organic linkers as ditopic, tritopic, and tetratopic ligands.[24–26]

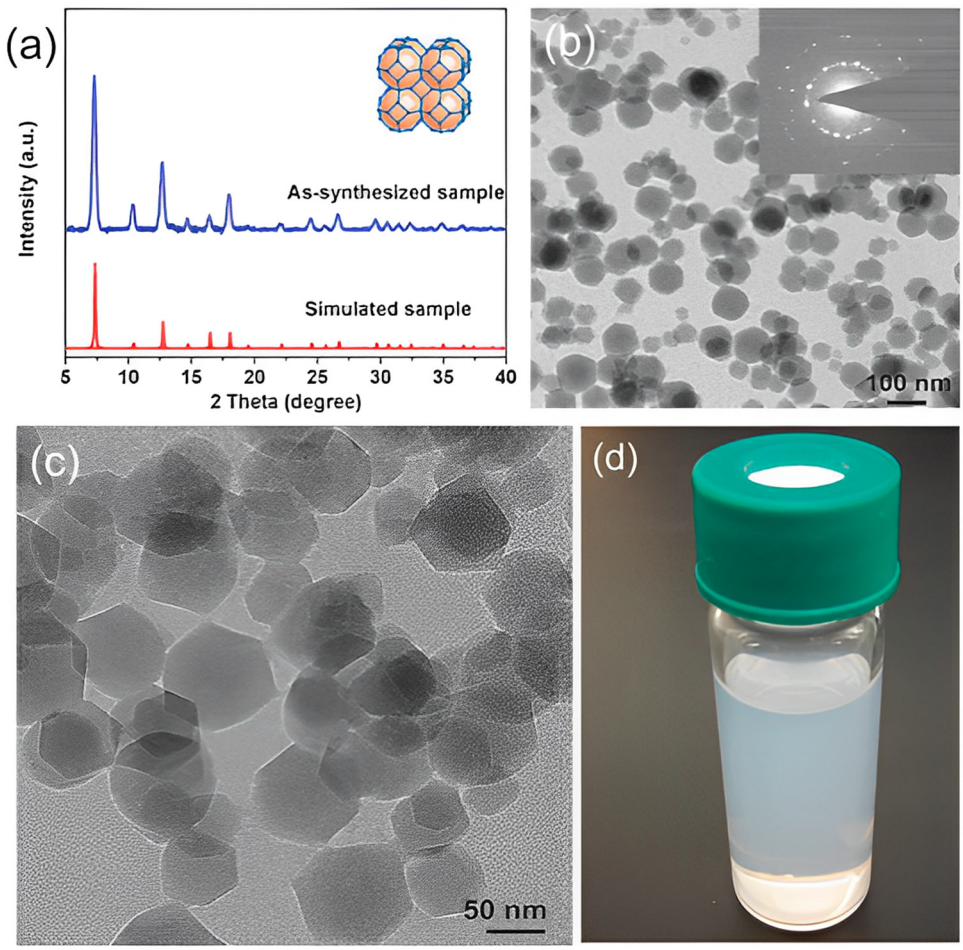

Fig. 3 (a) X-Ray diffraction patterns of ZIF-8 crystals. (b and c) Transmission electron microscope (TEM) images of ZIF-8 crystals. (d) Suspension of ZIF-8 crystals in methanol. Reproduced from ref. 14 with permission from the Royal Society of Chemistry, copyright 2017.

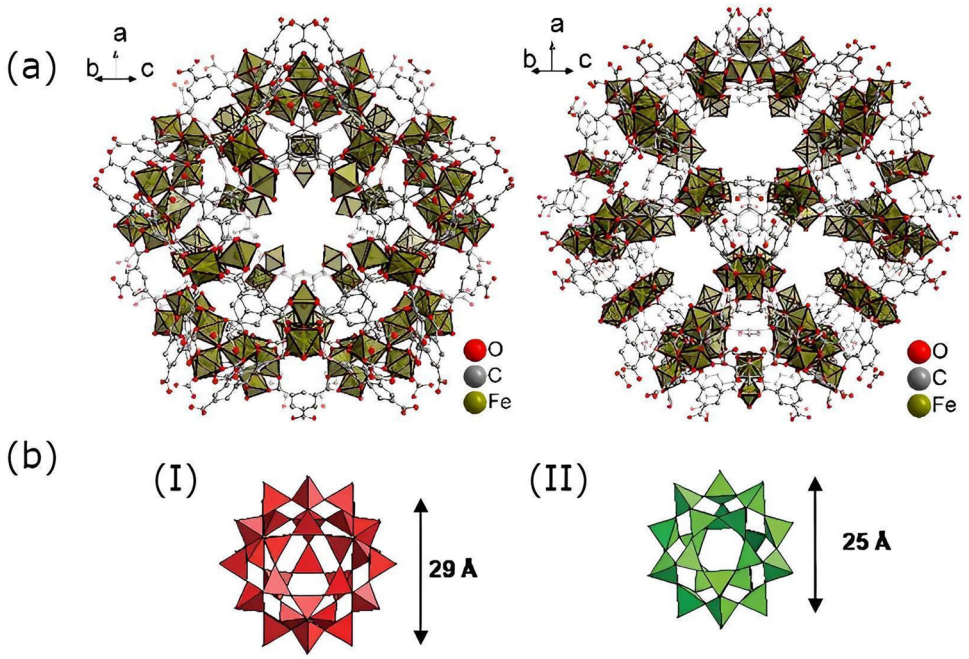

Fig. 4 (a) Structural frameworks of MIL-100(Fe) showing two distinct pore structures. Reproduced from ref. 19 with permission. (b) Different pore sizes in MIL-100(Fe): (I) hexagonal window and (II) pentagonal window. Reproduced from ref. 26 with permission from the Royal Society of Chemistry, copyright 2007.

MIL-100(Fe) is a type of Fe-based MOF with a tritopic ligand, benzene-1,3,5-tricarboxylic acid (BDC). It possesses a super tetrahedral structure due to the binding of trimesic acid and $[Fe_3(\mu_3\text{-}O)(COO)_6]$ secondary building units. As shown in Fig. 4, it has two different pore structures: a pentagonal window of 34 Å diameter and another hexagonal window with 29 Å diameter. It also exhibits a huge surface area as well as pore volume, allowing easy diffusion of substrates and molecules smaller than the pore window. MIL-100(Fe) is also endowed with distinctive properties such as thermal stability (stable in the air up to 280 °C and in N_2 up to 340 °C) and mesoporosity.[24–26]

MIL-53(Fe) is a medically important MOF and is iron(III) carboxylate based. It forms a "lozenge-shaped" pore system with a pore size that transitions from narrow to wide due to stimulation. This flexible structure allows for its use in drug loading and slow-release applications.[27]

The surface area and porosity of these materials find applications in drug loading and capturing of molecules. In medicine, MOFs find use in cancer detection and treatment in various ways as discussed in depth in the following sections inclusive of the photodynamic, sonodynamic, and theranostic applications.

2. Role of MOFs in the detection of cancer

Cancer detection is an area of research that requires much more attention since the early detection of cancer is essential for effective treatment. For this, highly sensitive tests are required that can detect tumors at early stages, especially with the help of identifying chemical biomarkers. Moreover, imaging techniques such as magnetic resonance imaging (MRI), computed tomography (CT-scan), X-rays, or ultrasound can be deployed for the study of tumorous growth in the body. Both the biomarker identification and the imaging techniques can be enhanced by the use of MOFs.

2.1 Biosensing

Sensing of tumors in living systems is performed through the identification of cancer biomarkers. These biomarkers are certain molecules that are released by tumor cells or produced by the defense system of the body in response to tumorous growth. The chemical nature of the biomarkers is variable and comprises a variety of molecules such as proteins, antigens, volatile organic compounds, microRNAs, and small metabolites that perform as cancer biomarkers.

The MOFs are chosen and modified in such a way that they bond with the specific cancer biomarker. These associated complexes can then be easily visualized through a number of spectroscopic techniques. A study on the concentration of these molecules in the sample can yield information about the severity of the disease. Since MOFs have a high surface area, they have ample sites for modification with molecules that interact with the biomarker. Though the biomarker itself can be used, the MOF structure allows for several such markers to be modified onto the MOF surface. Oftentimes, aptamers are utilized for the modification of MOFs, which are short chains of oligonucleotides or peptides that bind with the biomarker molecules. This integrated structure can then be detected which enhances the detection process and allows for recognition at low concentrations of the biomarker. This is essential in

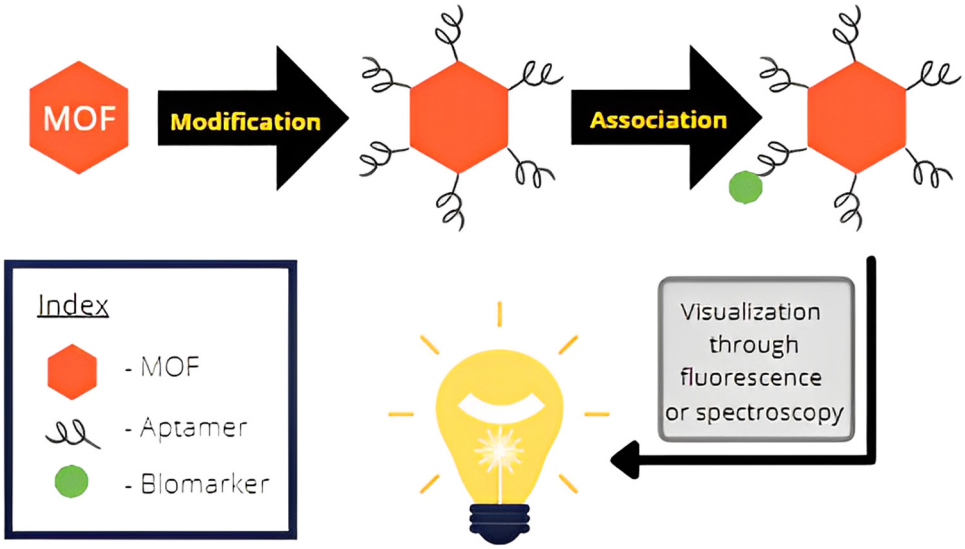

Fig. 5 Illustration showing the association of the biosensor molecule with the biomarker and subsequent visualization through spectroscopy.

the early diagnosis of cancers. Fig. 5 shows the generalized mechanism of biosensing through the assistance offered by MOFs.

Sheta *et al.* worked on liver cancer diagnosis through Cu-MOF-NPs[28] (Table 2, entry 1). The blood serum of healthy individuals was compared with that of patients suffering from hepatitis A, hepatitis B, and hepatitis C. Hepatitis patients are often at risk of hepatocellular carcinoma. The glycoprotein AFP (Alpha FetoProtein) functions as the biomarker in this case. The results were visualized through photoluminescence (PL) techniques. The results were like the ELISA results of the same patients.

Wang *et al.* employed a similar approach to analyze the blood serum samples of patients in their studies of ovarian cancers.[29] Carbohydrate antigen 125 (CA125) or Michigan cancer foundation-7 (MCF-7) cells functioned as biomarkers in this case. The results were visualized through fluorescence techniques. An integrated MOF-on-MOF structure was created. The Tb-MOF-on-Fe-MOF nanoarchitecture was linked with an aptamer molecule. This molecule served as a connecting link between the MOF architecture and the biomarker where the biomarker can be either CA125 or MCF-7 cells. In the presence of these biomarkers of ovarian cancer, the results were visualized through fluorescence techniques. The serum level of CA125 was below 35 U mL^{-1} in normal individuals but was elevated in the case of ovarian epithelial carcinoma (Table 2, entry 2).

MOFs have enhanced the early diagnosis of cancers. Qiao *et al.* studied early lung cancer diagnosis with the help of ZIF-8.[30] The core of GSPs (gold superparticles) was coated with a shell of ZIF-8 which was grafted with 4-ATP (4-aminothiophenol). 4-ATP reacts with the VOC 4-ethylbenzaldehyde which acts as a biomarker for lung cancer. VOCs can be identified from the exhaled breath of the patient. 4-Ethylbenzaldehyde is then identified through SERS (surface enhanced Raman scattering) spectroscopy, which can detect trace amounts of a molecule. Hence, this performs as an early lung cancer diagnosis technique (Table 2, entry 3).

A particularly interesting process of lung and breast cancer detection has been studied wherein "sandwich" oligonucleotide hybridization was employed for biomarker detection[31] (Table 2, entry 4), with the biomarker, in this case, being miRNA-155. A pair of oligonucleotide aptamer molecules were synthesized and attached to the surface of the Ag NPs and La-III MOF particles. The La-III MOF acts as a fluorophore while the Ag NP acts as a quencher upon association with the fluorophore. In the absence of a biomarker, the La-III MOF causes fluorescence through the

Table 2 Examples of MOFs in the detection and sensing of cancer biomarkers

Entry	MOF used	Target cancer	Biomarker of cancer	Biosensor	Findings	Ref.
1	Cu-MOF-NPs	Liver cancer	Alpha-fetoprotein (AFP)	Cu-MOF-NPs	Hepatitis patients were studied, and comparative data showed that the results were like the ELISA results of the same patients	28
2	Tb-MOF, Fe-MOF	Ovarian cancer	CA125, MCF-7 cells	Aptamer@Tb-MOF-on-Fe-MOF	Detection even at low concentrations of 58 μU mL^{-1} for CA125 and 19 cells per mL for MCF-7 cells. Essential for early detection	29
3	ZIF-8	Lung cancer	4-Ethylbenzaldehdye	4-ATP pre-grafted onto GSP@ZIF-8	Biomarkers (gaseous aldehydes) captured at 10 ppb limit of detection and hence provide an opportunity for early detection of lung cancer	30
4	La-III MOF	Lung cancer, breast cancer	miRNA-155	P1-aptamer@La-III MOF, P2-aptamer@Ag NPs	The fluorescent biosensor can detect low concentrations such as 0.04 ppb (ng mL^{-1}) or 5.5 fM of miRNA-155	31

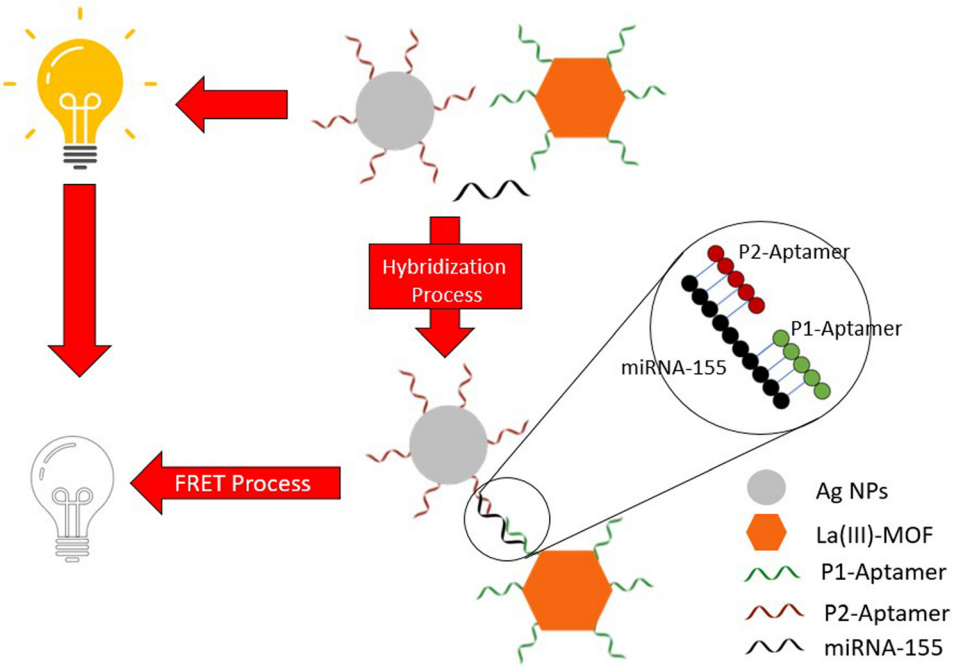

Fig. 6 Schematic showing the detection of miRNA-155 through "sandwich" oligonucleotide hybridization and simultaneous visualization through the FRET process. Reprinted (adapted) with permission from A. Afzalinia and M. Mirzaee, *ACS Appl Mater Interfaces*, 2020, **12**, 16076–16087, American Chemical Society, Copyright 2020.

FRET (fluorescence resonance energy transfer) process that can be observed. However, when miRNA-155 is present, it bonds to the two aptamer molecules hence forming a 'sandwich' structure that links the La-III MOF with the Ag NP with no fluorescence being observed in this case (Fig. 6). Hence, the lack of fluorescence marks the presence of cancer. Therefore, MOFs provide an overabundance of opportunities when it comes to detection techniques using biomarkers.

2.2 Bioimaging

Bioimaging techniques are useful in the *in vivo* visualization of tumors and they mainly comprise three basic options, namely magnetic resonance imaging (MRI), X-ray computed tomography (CT) scans, and optical imaging, and all of these can be augmented by the deployment of MOFs.

MOFs are metal-based materials and usually are transition metal-based. Transition metals are generally heavier atoms and their nature as such allows for higher contrast in imaging methods which require interaction with electromagnetic radiation. This has been applied in visualizing strategies *in vivo*.[32,33] Linkers of the MOF may also impart similar such attributes. Optical visualizing strategies work through fluorescence. MOFs excel in this application since their high surface area allows for suitable modifications comprising inclusion of carbon dots or other such fluorescent molecules. However, this strategy is mainly deployed in histological studies and investigations on cell cultures.[34]

MRI is a diagnostic tool that develops an image by detecting the nuclear spin reorientations in the presence of a magnetic field[22] and is achieved through the water molecules present inside the body. This technique helps to study and differentiate diseased tissues from healthy tissues. The deployment of MOFs of highly paramagnetic metal ions such as Gd(III), Fe(III), and Mn(II) enables the enhancement of the image contrast by causing an increase in the rate of water proton relaxation[35] (Table 3, entry 1).

CT is a method through which three-dimensional images are created through slices of X-ray images and is based on the properties of certain materials blocking the X-ray beam.[32] Generally, heavy ions such as iodine, bromine, or bismuth are administered to achieve better CT imaging. However, Lin *et al.* synthesized Cu(II) and Zn(II)-based MOFs that produced better results in CT scans than the conventionally used contrasting agent iodixanol[33] (Table 3, entry 2).

Table 3 MOFs utilized in optical imaging of cancer

Entry	MOF(s) used	Imaging method	Findings	Ref.
1	Gd(III), Fe(III) and Mn(II)	Magnetic resonance imaging	MRI is enhanced due to the improved image contrast by the increase of the rate of water proton relaxation	35
2	Cu(II) and Zn(II)	X-Ray computed tomography	CT is slightly enhanced since MOFs work better than the conventional contrasting agent iodixanol	33
3	UiO-66-NH_2	Fluorescence imaging	The MOF was modified with highly fluorescent carbon dots. This allowed for *in vivo* study of nanocarriers	34

Optical imaging is another technique for bioimaging that employs the use of luminescent dyes. There are two main strategies for the development of fluorescent MOFs. It can be accomplished either through incorporating luminescent ligands or *via* the introduction of luminescent dye groups in the ligands. Alijani *et al.* modified the UiO-66-NH_2 MOF with fluorescent carbon dots which enabled them to study the biodistribution of the drug-loaded MOFs *in vivo*.[34,36] The Fe_3O_4 core was coated with a shell of the MOF and this nanostructure was subsequently loaded with DOX and modified with carbon dots for deployment in breast cancer studies (Table 3, entry 3).

However, it should be noted that due to the problem of toxicity and financial constraints, MOFs are not exclusively deployed for imaging. They are often involved in a theranostic approach that simultaneously detects tumors and delivers the drug. These theranostic strategies have been discussed in the later sections.

3. Drug delivery

Metal–organic frameworks (MOFs) are extremely versatile nanostructures that are ideal vehicles for drug delivery and are superior to conventional chemical treatments which often affect healthy cells, thus causing alarming side effects. Therefore, specificity in delivering the drug is very crucial for a sustainable method of treatment. MOFs can be designed to be stimuli-responsive, a trait that can exploit physiological conditions like pH, temperature, and artificial aids to deliver the desired agents. Thus, they offer well-targeted and highly specific strategies which deliver the drug only to the affected cells. A few of these stimuli-induced principles have been discussed in this section (Table 4).

3.1 pH response-based drug delivery

The tumor microenvironments are known to be slightly more acidic than normal tissue because of hypoxia, inflammation, and glycolytic cell metabolism which can all affect blood flow. As illustrated in Fig. 7, the distinction between the pH of the healthy cells and cancer cells enables the MOFs to deliver the drug only to the tumor-specific region, as these drugs are simply released in an acidic environment, enabling an extremely selective and safe method of drug delivery. To date, the pH-stimulated mechanism remains the most well-researched and successful strategy for drug delivery through MOFs, with selected examples listed in Table 4.

The zinc-based MOF zeolitic imidazolate framework-8 (ZIF-8) is one of the most researched MOFs for drug delivery, due to its low cytotoxicity, porous nature, pH sensitivity, and superb drug loading capacity. Ozsoy *et al.* used ZIF-8 with bovine serum albumin (BSA) and boswellic acids (BAs) to synthesize the 5-sulfosalicylic acid/BSA/BAs@ZIF-8 MOF. The mechanism being pH-dependent exhibited over 75% drug release at pH 5 favoring micro-acidic environments. The thin ZIF-8 layer remained intact around the pH of normal cells (7.4) and broke down only under lower pH conditions ($\sim$5) ensuring drug delivery to only the cancer cells. BAs and BSA led to caspase 8 activation that caused apoptosis of cancer cells. This inhibits the inflammation regulatory complex NF-κβ in tumor cells, causing tumor death quickly and regression.[23] A similar pH-based mechanism was used to deliver doxorubicin (DOX), one of the well-known and used drugs in chemotherapy, that favored an ideal pH of 5.7–6.8. But DOX shows high levels of cytotoxicity which leads to various adverse side effects in the body. Therefore, a bio-MOF was formulated with chitosan (CS) coating to accomplish the delivery of DOX. A robust network of inter- and intrachain hydrogen bonds was created by the process, which required protonating the CS amine groups at lower pH values. This caused an open conformation and loaded the drug in the carrier. The technique was studied for the MCF-7 cell lines in breast cancer, and it displayed great performance and biocompatibility.[37]

Li *et al.* encapsulated dihydroartemisinin (DHA) in ZIF-8 nanoparticles *via* a one-pot encapsulation method; DHA is a semisynthetic derivative of artemisinin that exhibits strong antimalarial and anti-cancer properties. However, DHA is poorly soluble in water and displays poor bioavailability after oral administration[38] and this drawback has been significantly

Table 4 MOFs in drug delivery through the pH-stimulated mechanism

Entry	MOF used	Target cancer	Drug delivered	Findings	Ref.
1	ZIF-8	Breast cancer	5-Sulfosalicylic acid and boswellic acids (BAs)	The MOF showed pH-dependent drug release. The optimum release was found at acidic pH (5) with 75% efficiency over 10 hours, whereas no drug was released at neutral pH. Mechanistically, it was well-targeted and highly efficient against breast cancer cells	23
2	Bio-MOF-13-Co	Breast cancer	Doxorubicin (DOX)	93% of the anticancer drug DOX was ideally released at pH 6.8 within 48 hours. Slow release without any burst effects was observed. Free DOX displayed greater cell mortality	37
3	ZIF-8	Liver cancer	Dihydroartemisinin (DHA)	DHA encapsulation efficiency was found to be 77.2% and 75.7% of the drug was released successfully at pH 5.5. Resulted in apoptosis of cancer cells by the p53 mediated mitochondrial pathway and inhibited glycolysis *via* PI3K/AKT signaling	39
4	ZIF-8	Liver cancer	Curcumin	HepG2 cell lines were studied, and effective drug delivery (73.1%) was found to occur at pH 5. The MOF nanocarrier led to faster delivery and greater bioavailability of curcumin to the body cells	42
5	$[Gd(BCB)(DMF)](H_2O)_2$	Liver cancer	5-Fluorouracil (5-Fu)	Controlled and progressive drug release was observed (68%) within 20 hours, at around pH 6.5	44

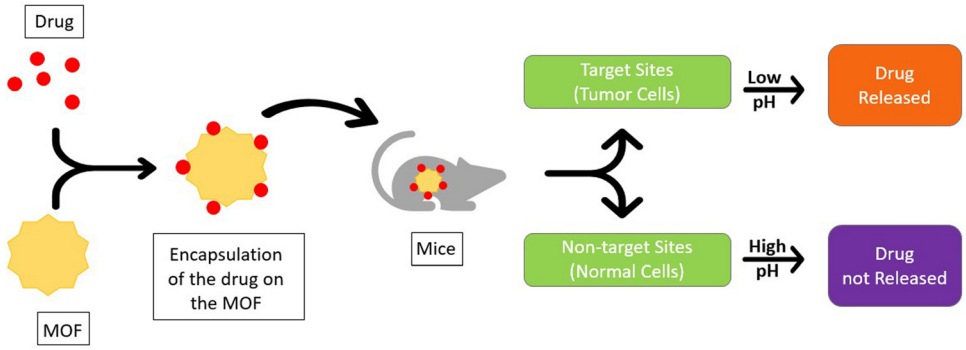

Fig. 7 Mechanistic pathway of pH-based drug delivery using MOFs.

circumvented by the DHA@ZIF-8 MOF. The ensued MOF displays great drug loading capability, encapsulation efficiency, and biocompatibility with sustained drug release favoring acidic microenvironments and inhibiting tumors more successfully (smaller tumor size and higher inhibition rates) than the free DHA. The mechanism, shown in Fig. 8, involves various pathways, including MAPK signaling, PI3K-AKT, p53, glycine, serine, and threonine[39] wherein DHA inhibits the PI3K/AKT signaling pathways linked to cell proliferation, survival, and cancer progression;[40] p53 and PI3K/AKT pathways are interrelated. PI3K/AKT negatively regulates the p53 levels by causing the transport of oncoprotein M2D2 into the cell nucleus. Transcriptional activation of tumor suppressor genes like PTEN inhibits the MDM2 translocation, weakening the PI3K/AKT signaling and further increasing the p53 levels.[41,42] The p53 pathway induces the Bcl-2 family member Bax, as well as the BH3-only proteins Bid, Puma, and Noxa. The inhibition of the PI3K/AKT pathway decreases the metabolism of glucose in cells by inhibiting HIF-1α and reduces the expression of crucial glycolytic enzymes such as PMK2, LDH, and Glut, thus decreasing the glycolysis/gluconeogenesis in cancer cells.[43]

MOFs can be exploited to deliver natural agents as drugs. One such example is the extremely common and beneficial naturally occurring organic molecule curcumin (CCM) which is known for offering the bright yellow color of turmeric, popular for its antioxidant, anticancer, antibacterial, and anti-inflammatory properties for ages. But its hydrophobic nature presents a problem to use curcumin directly as a drug in the affected location. Xiao and his team solved this problem through the incorporation of curcumin in the MOF CCM@ZIF-8&α-lip, made up of Zn^{2+} ions, α-lipoic acid (a natural antioxidant produced by our body, also found in various food sources), and curcumin (CCM) encapsulated in the MOF as the drug. The experiments performed on the HepG2 cells of mice showed optimum drug delivery at a pH of 5.0, which is the common pH for tumor cells. The pH specificity ensured that

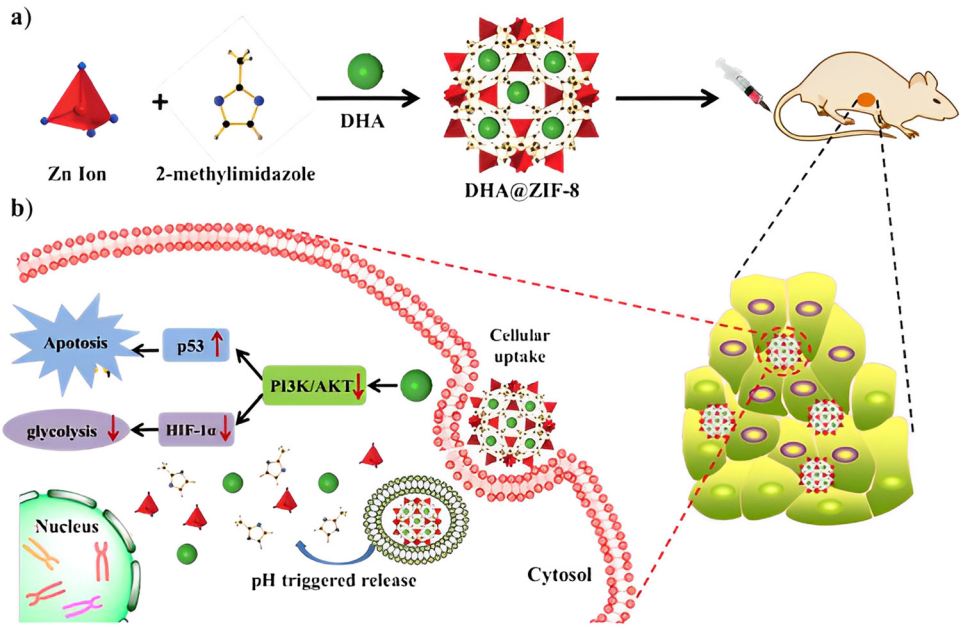

Fig. 8 (a) Preparation of DHA@ZIF-8 NPs and (b) mechanism of drug action of DHA in HepG2 cells. Reproduced from ref. 39 with permission from the Royal Society of Chemistry, copyright 2020.

the drug was only released to the cancer-affected cells and not to the normal cells.[42]

Recent studies introduced the possibility of using group-f elements in MOFs. One such is the gadolinium (Gd) based MOF $[Gd(BCB)(DMF)](H_2O)_2$, with 4,4′,4″-benzenetricarbonyltribenzoic acid (H_3BCB) as the organic linker and a metal node-based 1D Gd(III) secondary building unit chain. The drug release was optimum at pH 6.5, favoring slightly acidic conditions thus mimicking the cancer environment with *ca.* 68% efficiency. Furthermore, cell viability was found to be over 80% and hence the carrier was nontoxic to body cells even with concentrations exceeding 200 μg mL^{-1}, proving the excellent biocompatibility of the drug-loaded MOF.[44]

3.2 Magnetic response-based drug delivery

While the pH-responsive MOFs hold the most substantial position in drug delivery practices, magnetic behavior-stimulated delivery stands as a lesser explored option. It is an effective technique that enables the precise delivery of the desired drug to the tumor sites selectively. Drug carrier systems are prepared by incorporating a suitable MOF with magnetic constituent particles along with a prospective drug. When a magnetic field from outside is applied, the magnetic moieties in the MOF cause the drug molecules to align according to the field and ensure highly localized delivery of the drug to the tumor sites. The magnetic stimuli can assist in maintaining a stabilized concentration of the drug in the target tissue over a long time without the risk of dispersion to the healthy cells and circulation through the bloodstream. MOFs based on paramagnetic metals like Fe, Co, Ni, and Mn, which show important magnetic behaviors like low coercivity, high magnetic susceptibility, and superparamagnetism, are highly preferred for the role of delivery vehicles; the common examples are mentioned in Table 5.

Sethi *et al.* prepared Fe-based nanoscale MOFs with different coordinating solvents wherein Nile Red was used as the organic hydrophobic dye and doxorubicin hydrochloride (DOX) was the loaded drug. Characterization of the MOFs through transmission electron microscopy, probing, and advanced spectroscopic techniques revealed that the MOF prepared with DMF as the coordinating agent possesses high saturation magnetization, superparamagnetism, and negligible coercivity. Analysis of the drug release profile over 15 days showed a maximum release of 88% drug, with a sustainable delivery pattern without any burst release effects and precautious detonation. *In vitro* studies confirmed the excellent uptake of DOX by the target cells which can be further improved by treatment with a strong external magnetic field.[45]

The controlled drug release behavior in magnetically aided MOFs was also shown by Ke *et al.* with their preparation of

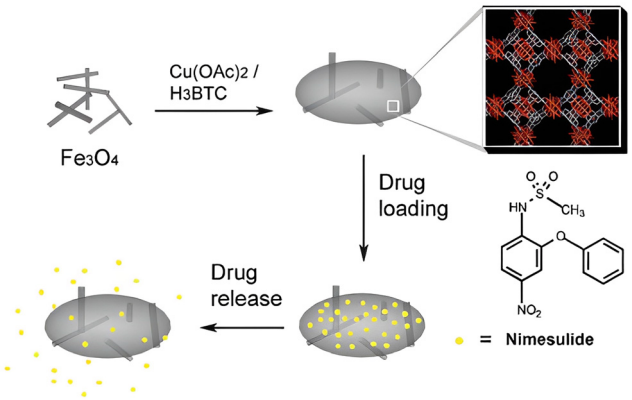

Fig. 9 $Fe_3O_4/Cu_3(BTC)_2$ MOF-based delivery of nimesulide (NIM). Reproduced from ref. 46 with permission from the Royal Society of Chemistry, copyright 2011.

$Fe_3O_4/Cu_3(BTC)_2$ magnetic nanocomposites by incorporating Fe_3O_4 nanorods with $Cu_3(BTC)_2$ nanocrystals. Nimesulide (NIM), a nonsteroidal anti-inflammatory and anti-cancer drug, widely used for pancreatic cancer treatment, was well absorbed (0.2 g per gram composite) by this novel MOF, followed by a slow and sustained delivery of the complete drug over a period of 11 days in physiological saline at 37 °C (Fig. 9). [46] Similar results were demonstrated by Wu and his colleagues by fabricating magnetic γ-Fe_2O_3 nanoparticles on MIL-53(Al) through *in situ* pyrolysis synthesis. The controlled release of ibuprofen was perceived, and after 7 days in physiological saline maintained at 37 °C, the drug was fully released.[47]

3.3 Temperature response-based drug delivery

Understanding the thermal kinetics of MOFs is another step toward harnessing maximum efficiency and compatibility in drug delivery. Many MOFs such as those listed in Table 6 are found to be thermosensitive where temperature plays a crucial role in regulating the pore size of the drug carrier. Depending upon the pore modification, high temperatures can either increase the drug delivery rate or even delay its release. Most studies are concentrated on zinc and zirconium-based MOFs, as they are generally preferred for their high thermostability and chemically stable properties. At the same time, these MOFs exhibit great porosity, reflecting on their ideal drug-carrying capacity, and are also known to be biocompatible to a large extent. Such a mechanism based on thermal stimuli was formulated by Nagata and the team in 2012, which was also one of the earliest published works on drug delivery through thermal regulations. They successfully created a smart MOF by

Table 5 MOFs in drug delivery through magnetic stimulation

Entry	MOF used	Drug delivered	Findings	Ref.
1	F-NMOF	Doxorubicin	Slow, sustainable, and efficient drug release was seen; 88% of the drug was released within a period of 15 days. Cell viability analysis confirmed the nontoxicity of the drug-loaded MOF	45
2	$Fe_3O_4/Cu_3(BTC)2$	Nimesulide (NIM)	The drug was released in a slow and controlled manner over a period of 11 days	46
3	MIL-53(Al)	Ibuprofen	Very slow and gradual release patterns were seen within 5 days	47

Table 6 MOFs in drug delivery through the temperature-stimulated mechanism

Entry	MOF used	Drug delivered	Findings	Ref.
1	JZU-64	Methotrexate (MTX)	The MOF showed around 63% drug release rate after 8 hours at 60 °C, much higher than the delivery rate at normal body temperature, *i.e.* 37 °C	36
2	JZU-801	Diclofenac sodium (DS)	More than 90% drug was released at the end of 25 hours in local hyperthermia tissues at 60 °C	48
3	NU-1000	Calcein, α-cyano-4-hydroxycinnamic acid (α-CHC)	The release rate of calcein and α -cyano-4-hydroxycinnamic acid (α-CHC) was slowed down by temperature treatment	49

modification with a thermoresponsive polymer (PNIPAM) on its surface that operated on a simple ''ON–OFF'' principle.[36]

Recently, there have been widespread studies analyzing the effect of temperature in delivering drugs through MOFs for therapeutic purposes. Methotrexate (MTX), a prominent anti-cancer and anti-inflammatory drug, was incorporated into the zinc-based porous MOF ZJU-64; drug release was found to be ~68.3% at 60 °C under the hyperthermic condition in 8 hours. Compared to normal body temperature (37 °C), the drug release was much accelerated. The quantity of MTX delivered at 37 °C in 72 hours could be compared to the amount delivered in just 1.5 hours at 60 °C.[36] Jiang *et al.* reached similar outcomes of accelerated delivery as well when they encapsulated diclofenac sodium (DS), a powerful non-steroidal anti-inflammatory drug (NSAID), in ZJU-801, a zinc-based MOF. At 60 °C, the maximum release rate was recorded. This temperature was 3.4 times greater than that of 37 °C and about 10.3 times higher than that of 25 °C.[48] On the other side of the spectrum, Teplensky *et al.* showed that higher temperature modification can lead to delayed and consistent drug delivery. Temperature treatment of the MOF NU-1000, above 180 °C, resulted in partial pore collapse of the MOF, which entrapped the chosen drug, calcein, and delayed its release by 7 days. Temperature treatment also decreased the cell viability in the case of α-cyano-4-hydroxycinnamic acid (α-CHC) encapsulated NU1000. After incubation of 48 hours, the viability further dropped with the rise in drug concentration, resulting in almost 0 viability at *ca.* 1.6 mg mL^{-1} drug concentration. The effect of the non-temperature treated sample and the free drug on cell viability was much less pronounced.[49]

4. Therapeutic practices

4.1 Chemotherapy

Chemotherapy is considered a prevailing helpful methodology due to its high efficiency compared to others. The development of novel advanced techniques for synchronous cancer diagnosis and treatment has been an important biomedical research field in the past few decades to meet the developing needs for cancer monitoring and the growing clinical need for therapies as well. Among various cancer treatments, chemotherapy is a vital choice for most cancer cases because of its high efficiency. Artemisinin (ART) is a natural drug with potent anticancer activities, and unlike other chemical-based anticancer drugs, such as DOX and PTX (paclitaxel), it exhibits reduced side effects and lower chance of metastasis and recurrence.[50,51]

Chemo sessions include various therapies to shrink tumors or destroy the remaining cancer cells. Basically, these sessions are to treat cancers of the blood or lymphatic systems such as leukemia and lymphoma. Most conventional cancer treatments comprise chemotherapy, radiotherapy, and surgery, in which patients may endure genuine side effects and unsatisfactory treatment results.[52] Due to these failures, there has been a shift in emerging therapies for cancer treatment, such as immunotherapy, gene therapy, and photothermal therapy (PTT), which have progressed well and have potentially enhanced the therapeutic outcomes (Table 7).

4.1.1 Photothermal therapy. Photothermal therapy utilizes near-infrared (NIR) laser-induced thermal removal of cancer cells which has been widely explored and shown superb combined helpful impacts when applied together with common chemotherapy and other modalities. The photothermal transformation impact begins with the charge transfer transition between Fe(II) and Fe(III). Also, it has been shown from the previous reports that PB@MIL-53(Fe) nanocubes are prepared through layer-by-layer growth of MIL-53(Fe) shells for pH-responsive chemotherapy and PTT.[53,54] Amongst different theranostic technologies detailed so far, photoacoustic imaging (PAI) combined with photothermal therapy (PTT; PAI/PTT) was found to be a capable photo theranostic tool for cancer diagnosis and treatment. In PAI/PTT, the therapeutic benefits were offered by photothermal therapy (PTT), while the diagnosis was based on photoacoustic imaging (PAI).

Table 7 Applications of MOFs in advanced chemotherapy, photothermal therapy, and other combination treatments

Entry	MOF used	Target	Findings	Ref.
1	Fe-MIL-101	Ovarian cancer	Exhibited stronger antiangiogenic effects toward HUVEC cells than the anti-angiogenic inhibitor.	52
2	ZIF-8	Combination therapy	CSD-MOF crystals loaded with the anticancer drug doxorubicin (DOX) are efficient pH and near-infrared (NIR) dual stimuli-responsive drug delivery vehicles	50
3	sMoSe2-ICG NSs	Photothermal therapy	Phototheranostic technology based on photoacoustic imaging (PAI) is emerging as a powerful tool for theranostic application	56
4	DOX and PTX	Anticancer drugs	Chemotherapeutic agents require the presence of hydrophobic patches and a flexible fold could probably make alpha-lactalbumin a suitable carrier for hydrophobic drugs	54

PTT is a highly favored therapeutic modality because it is non-invasive and highly selective. Moreover, a photothermal agent is exploited to absorb near-infrared (NIR) light and convert it into cytotoxic heat to kill cancer cells.[54,55]

While considering all these explorations, the synthesis of various PB@MIL-53(Fe) dual-MOF structures has been accomplished as they offer effective dual-mode therapeutic agents which efficiently combine photothermal therapy and chemotherapy. In addition to the inner PB MOFs and the outer MIL-53(Fe), MOFs can serve separately as T2 MRI and T1/T2 differentiate specialists. The combination of MR and FOI dual-mode imaging-guided therapy can yield complementary diagnostic data and offer synergistic focal points over single-modality-guided theranostics.[56] These d-MOFs can load the hydrophobic anticancer drug ART with a high loading content of 848.4 mg g^{-1}. More importantly, the outer MOF of the prepared PB@MIL53(Fe) can collapse in acidic environments to release the load. Also, ART-loaded dual-mode MOFs can be utilized for combined photothermal therapy and chemotherapy, which reveal synergistic effects not only in *in vitro* cell culture assays but also in a mouse tumor model.[57]

4.1.2 Starvation therapy. Cancer starvation therapy is emerging as a compelling strategy for suppressing tumor growth and survival by blocking the blood flow or depriving the basic supplements of tumors. The transport of supplements may be blocked by halting the tumor blood supply with the medications of angiogenesis-inhibiting agents (AIAs), vascular disrupting agents (VDAs), and trans arterial chemoembolization (TACE). Besides, specialists that may expend the intratumoral nutrients or intervene with the uptake of fundamental substances by tumor cells can also lead to tumor starvation and necrosis.[53] The advances in nanotechnology, as well as cancer biology, have boosted the development of drug delivery systems for cancer management with enhanced efficacy and constrained side effects. Among them, a variety of nanomaterials based on natural/synthetic polymers, liposomes, MOFs, gold nanoparticles (AuNPs), and silica NPs have been employed to co-deliver cancer-starving agents and other therapeutics with the aim of reducing the side effects, improving their targeting efficacy, increasing the stability and half-life of therapeutics, and co-delivery of multiple drugs to overcome drug resistance. Furthermore, as depicted in Fig. 10, cancer starvation strategies related to multimodal nanomedicines have been created for accomplishing synergistic cancer therapy, which has been illustrated to be an efficient way of overcoming the side effects of free drugs, thus resulting in superadditive therapeutic effects.

Most of the time, combined chemotherapy or combination therapy *i.e.*, chemotherapy plus gene therapy, also operates on these MOFs with the aim of enhancing the therapeutic index of drugs and reducing toxicity by using various combinations of drug molecules. 5 year survival rates are still quite low for most

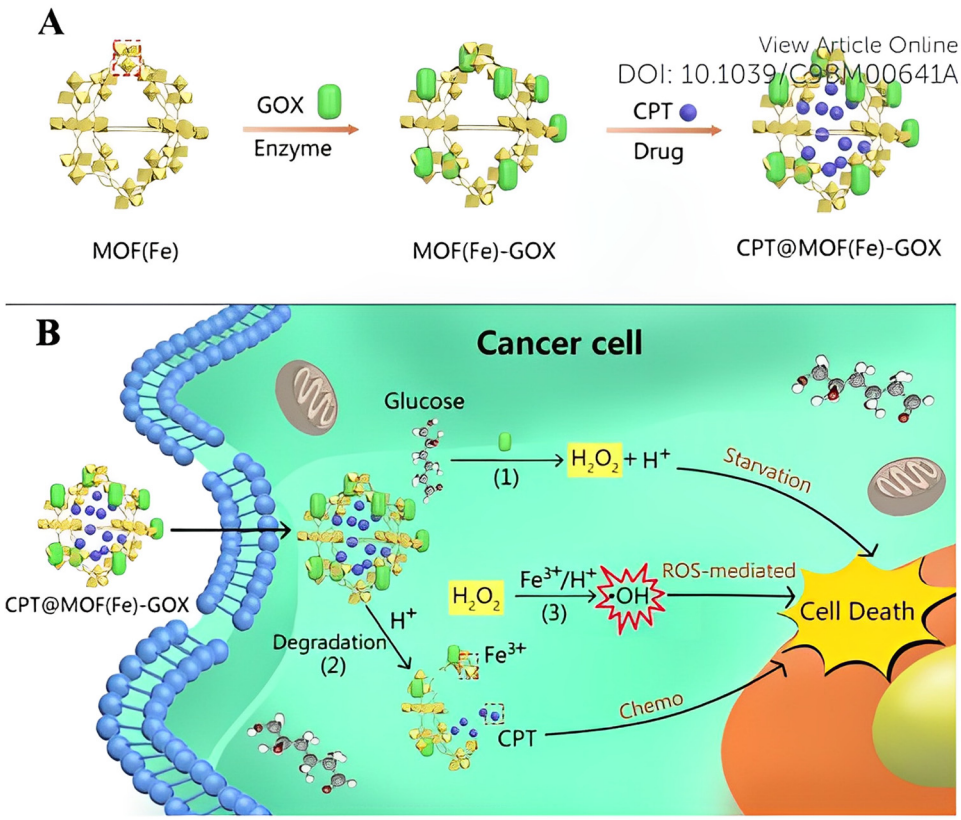

Fig. 10 (A) Surface modification of the GOX enzyme and uptake of the CPT drug by Fe-MOF. (B) Schematic representation of cascade reaction activated synergistic cancer starvation/ROS-mediated/chemotherapy based on CPT@MOF(Fe)-GOX particles in HeLa cells. Reproduced from ref. 55 with permission from the Royal Society of Chemistry, copyright 2019.

metastatic cancers, and the process of developing a new cancer drug is costly and extremely time-consuming. Therefore, new techniques that target survived tumor and provide effective results at a reasonable cost can be considered for treatment. But all these approaches can only work when the FDA-approved agent targets the same pathways of survival. One such example has been in the combination therapy arena which targeted a drug that has been already FDA-approved and where the overall cost also has been reduced.[55]

Therefore, diverse aspects of MOFs and drugs are still there to be explored for various therapies performed in cancer treatment, and hopefully, this review stimulates the thinking process for the newer survival pathways with effective results.

4.2 Photodynamic therapy

Photodynamic therapy (PDT) is a combination of three different non-toxic units which work together in the apoptosis of the target cell, the three components being a photosensitizer (PS), light, and oxygen. They combine to produce reactive oxygen species (ROS), which help in the apoptosis of cells. PDT also helps in decreasing the damage to non-target cells by localizing the delivery of the PS and light. Hence, PDT is being adapted to treat cancer in recent years.[58]

Firstly, the PS absorbs light energy and transforms into an excited triplet state from a singlet state. Then the PS responds to light *via* two different pathways. In the Type I pathway, superoxide anion radicals (O_2^-) and hydroxyl radicals are produced when the PS reacts with triplet oxygen ($^3O_2$) or water. On the other hand, in the Type II pathway,– the PS generates cytotoxic singlet oxygen ($^1O_2$) by transferring its energy to the surrounding $^3O_2$. Type I PDT shows hypoxia tolerance and Type II PDT indicates high reactivity and the combination of both could be a significant move in applications for PDT.[59] MOFs are additionally highly adjustable and structurally and functionally tunable, making them ideal for drug delivery and also for controlled release.[58] Therefore, the usage of nanoscale metal–organic frameworks (NMOFs) as PSs can prove to be successful in treatments (Table 8).

The usage of nanoparticles has been viewed as an alternative to the normal delivery of PSs to enhance the efficiency of PDT. However, due to the failure in the optimization of the production of ROS and their transport to intracellular organelles to kill cancer cells, nanoparticles have shown only low success in PDT. MOFs, being a class of blend materials comprised of metal ions and multiple organic linkers, have shown more success in PDT due to their high stability and other exceptional properties.

Lu *et al.* used a porphyrin-based NMOF, DBP-UiO, as a PS in PDT, which exhibited high stability under aqueous conditions and its 5,15-di(*p*-benzoato)porphyrin (DBP) ligands were neatly separated from others, thus preventing self-quenching. The $^1O_2$ generation efficiency increased due to the Hf^{4+} ions which coordinated with the carboxylate groups of ligands of the DBP which enhanced the intersystem crossing (ISC). Even though the performance in pilot animal studies was immense, chlorin-based NMOF-DBC-UiO was developed as the photophysical properties of DBP-UiO were not very favorable. This shows that the stability of NMOFs alone may not be efficient for treatment in PDT; higher photophysical properties are additionally needed. Since DBC-UiO had improved photophysical properties, it showed better PDT efficiency in colon cancer mouse models. The photophysical properties of the chlorin-based PS were confirmed by UV-vis absorption spectroscopy. The use of the singlet oxygen sensor green (SOSG) probe revealed that NMOF-DBC-UiO was three times more efficient than DBP-UiO in total $^1O_2$ generation.[58]

Some tumor sites are hypoxic affecting the efficiency of PDT; therefore new PSs that show high photosensitivity may be required. A MOF that could increase oxygen levels in hypoxic environments to augment the conversion of O_2 to ROS and which enhances the PDT efficiency could be of great significance under these conditions. As shown in Fig. 11, manganese oxide can catalyze the production of oxygen from hydrogen peroxide, and as a result, Mn-MOF can be used for increasing O_2 levels and at the same time be deployed as a PS to enhance PDT. H_2O_2 can be decomposed by the active center Mn(II) to produce O_2 which can then be used to sensitize oxygen and then produce ROS. It should be noted that the production of O_2 in cancer cells is catalysed by Mn-MOF; Mn-MOF deployed on breast cancer tumors in mice significantly increased the O_2 concentration which led to the strengthening of PDT. To check the efficiency of Mn-MOF it was compared with Al-MOF, under normal oxygen conditions and hypoxic conditions. Under normal oxygen conditions, after being irradiated by light for a period, the fluorescence intensity of the cells was comparatively increased which indicated that both MOFs can produce ROS in normal cells. On the other hand, under low oxygenic conditions, Mn-MOF showed greater fluorescence intensity which indicated that it has a better ability to increase ROS levels in hypoxic cells.[60]

Table 8 Role of MOFs in photodynamic therapy

Entry	MOF used	Target organ	Type of PDT	Findings	Ref.
1	DBC-UiO	Colon	Type II	The experiments showed 3 times increased singlet oxygen production compared to porphyrin based MOF previously used due to the high photodynamic properties of chlorin	58
2	UMOF-TiO_2	Hypoxic tumors	Type I and II	For the apoptosis of complex tumors, both Type I and II have been used here. Titanium oxide functions as a photocatalyst making this MOF produce more ROS than UMOF alone due to the presence of light	59
3	Mn-MOF	Breast	Type II	Mn in this MOF helped in producing oxygen required in hypoxic tumors from hydrogen peroxide. Compared with Al-MOF, Mn-MOF showed great potential under the hypoxic conditions of tumors for producing ROS	60

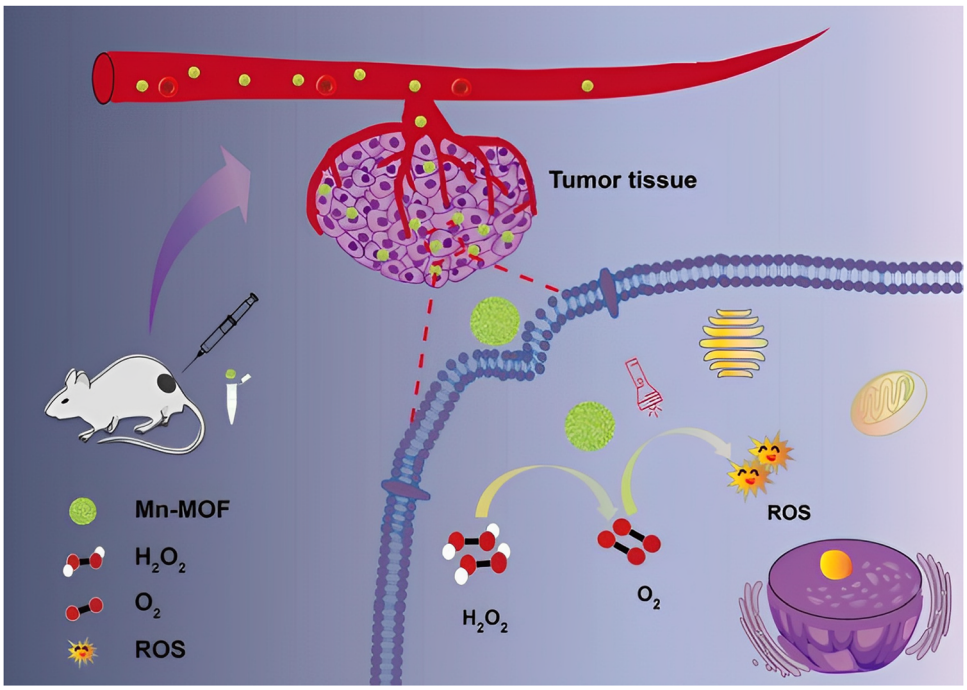

Fig. 11 Photodynamic therapy exhibited by Mn-MOF. Reproduced from ref. 60 with permission from the Royal Society of Chemistry, copyright 2019.

To check the efficacies of these MOFs in treatments, they were evaluated on different cancer cells. DBC-UiO was tested on colorectal cancer of murine and humans, and Mn-MOF was tested on a mouse breast tumor model.

In colorectal cancer, the *in vitro* PDT efficacies were investigated by comparing DBC-UiO against DBP-UiO and the corresponding free ligands. The result showed that DBC-UiO performed better than DBP-UiO by eliminating the cancer cells effectively at low NMOF and light dosages. In addition to it, the *in vivo* efficacy against cancer in tumor mouse models was examined. DBC-UiO inhibited the growth of the tumor but DBP-UiO failed to suppress the growth of the tumor at lower doses of PS and light. To confirm the treatment, the histology of slices of the frozen tumor showed that DBC-UiO gave grounds for apoptosis or necrosis of tumors.[58]

In the breast tumor model of mice, Mn-MOF was compared with a control group. After 14 days, the tumor in the control group showed an increase in volume but the tumor treated with Mn-MOF showed almost no change in the mice. The tumor volume also turned out to be significantly smaller in the treatment group compared to that of the control group proving that Mn-MOF can improve the PDT even under low oxygenic conditions. To verify it further, the efficacy of PBS, PBS + laser, Al-MOF, Al-MOF + laser, Mn-MOF, and Mn-MOF + laser, respectively, was also examined. After the treatment of 14 days, no significant change in weight was noticed.

The volume of the tumor in the Mn-MOF + laser group was lesser than that in the Al-MOF + laser group which indicated the greater efficacy of Mn-MOF *in vivo*. Mn-MOF was injected directly into the section with the tumor and it showed less influence on other organs which also specified the low toxicity of Mn-MOF *in vivo*.[60]

The above treatments showed only Type II PDT. To enhance the efficiency in some complex tumor models, both Type I and Type II have to be used.

A different nanomaterial – lanthanide-doped upconversion nanoparticles (UCNPs) – was identified as an excellent material with anti-Stokes emission properties even when excited under low-power light. UCNPs due to their potential to convert high tissue-penetrating near IR and UV light can be used as *in vivo* light modulators causing minimum photodamage due to the enhancement of PDT. Titanium dioxide (TiO_2) which can function as a photocatalytic semi-conductor with UV light and its chemical stability has been exploited extensively in the platform of theranostics for PDT. Since UV light promotes the production of photogenerated electrons and holes from TiO_2 which in turn react with the neighboring medium to produce a lot of ROSs, the combination of UNCPs and TiO_2 could attain multimode PDT and will show a powerful result due to its flexible modification.

Shi and his team created a nanoplatform based on a heterodimer comprising UCNPs and meso-tetra(4-carboxyphenyl)porphine (TCPP)-MOF which was also enclosed with ultra-small TiO_2 nanoparticles (UMOF-TiO_2). This UMOF-TiO_2 could achieve both Type I and Type II PDT and could be activated by a 980 nm near-infrared (NIR) laser. It efficiently produced various cytotoxic ROS and induced the apoptosis of cancer cells *in vitro* and *in vivo*, when it was exposed to the 980 nm laser. It was uncovered that UMOF-TiO_2 produced a large amount of ROS and it generated more ROS than UMOF which could have been because of the loading of TiO_2 before the utilization of light. All the results in the different tests showed that the synthesized nanomaterials could generate $^1O_2$, $O_2^{\cdot-}$ and OH which enabled the

amalgamation of both Type I and Type II PDTs. It also revealed good biocompatibility and better cytotoxicity compared to unirradiated UMOF-TiO_2 indicating increased potency. These results show that UMOF-TiO_2 is a superior PS that when used *in vivo* can show the great function of tumor PDT.

Further, nude mice were divided into random 4 groups and treated differently. The groups which were treated with UMOF-TiO_2 under irradiation showed the most significant reduction in tumor volume. The same treatment displayed an increase in tumor size over time when it was not open to the light. These changes in the volumes of tumors indicated the fabulous work of UMOF-TiO_2 as a photodynamic reagent. Furthermore, blood routines and biochemical index analysis showed no significant difference in the hepatic or renal function markers and several others even after treatment of 14 days. Also, UMOF-TiO_2 indicated high histocompatibility. This showed the excellent potential of this nanomaterial for application in the biomedical field. Different treatments have been deployed depending on the different types of cancers due to the difference in the ability of oxygen for PDT. Therefore, the treatments are very selective for different tumors.

4.3 Sonodynamic therapy

Sonodynamic therapy (SDT) is another effective way of cancer therapy that has been developed from photodynamic therapy. Like PDT, it is a non-invasive therapy and plays a huge role in the treatment of hypoxic tumors.[61] While PDT can be very effective in certain cancer types, it may be very limited in treating tumors that are hypoxic like pancreatic cancer due to the dependency on oxygen for the treatment of biological tissues.[62] The stimulation of ultrasound (US) for triggering the sonosensitizer mediates ROS generation ($^1O_2$) and actuates the cellular damage. As a result, SDT is primarily dependent on the intratumoral availability of oxygen for ROS generation and shows a requirement for a molecule that can be activated under US to generate oxygen.[63] One such molecule that showed US responsiveness is titanium dioxide nanomaterials (TiO_2). Like PDT this also could show Type I SDT by producing cytotoxic radicals and superoxides due to the stimulation by US. However, the TiO_2 materials are unstable and have limited energy transfer efficiency. The surface of TiO_2 is unstable and reacts with the surroundings upon irradiation resulting in a low yield of ROS. This requires the design of a stable carbon-coated sonosensitizer that generates oxygen in an efficient manner even in an oxygen-independent environment. Cao *et al.* developed such a MOF TiO_2/C nanocomposite that showed excellent stability and also proper ROS generation when responding to the US stimulation under hypoxic conditions.[62]

Another problem seen in SDT enhancement is the use of hypoxia-activated anti-cancer drugs combined with sonosensitizers. However, it does not foresee the scarcity of O_2 in tumors which results in decreased susceptibility, reduced target sites, and drug-resistant gene expression. Pan *et al.* prepared a double-layer hollow manganese silicate nanoparticle (DHMS) derived from a MOF. Since the Mn element could be oxidized by holes exposed to US irradiation, DHMS could generate a large number of $^1O_2$ and hydroxyl radicals ($^\bullet$OH). It possessed a great ability that let itself produce O_2 by reacting with endogenous H_2O_2 which increased the efficiency of SDT. TiO_2 was used in animal studies to test *in vivo* efficiency. Mice were assigned and were subcutaneously implanted with Panc02 cells which established tumors. The results confirmed after repeated SDT that TiO_2/C was stable and confirmed its ability to generate ROS nonstop to successfully achieve anti-tumor efficacy. It also showed that TiO_2/C generates cytotoxic radicals including O_2^-, H_2O_2, and $^\bullet$OH which makes it Type I SDT.[62] The DHMS used on mice also showed excellent results. The inhibition rate of the tumor was around 92.0% and it could be noted that DHMS with US-mediated SDT induced remarkable necrosis and apoptosis of cancer cells in the tumor without obvious side effects on major organs.[63]

5. Theranostic applications

In medicine, theranostics is a novel way of integrating therapy and diagnostic techniques, which allows us to detect the anomaly and deliver the required therapeutic treatment to the target site at the same time. Modern treatments often come with a cost; therefore developing novel synergistic techniques is the need of the hour. Multimodal imaging is the combination of multiple molecular imaging strategies to provide early detection, timely feedback, and the exact localization of cancer. Although monomodal molecular imaging techniques like MRI, CT, PAI, *etc.*, are efficient for cancer diagnosis to an extent, they have their own set of limitations. As shown in Fig. 12, administering two or more imaging procedures together with therapeutic treatments like chemotherapy, photothermal therapy or photodynamic therapy is a sustainable way to circumvent individual shortcomings that allow us to receive optimum results with minimal one-time efforts. Research continues to explore this field today for constructing ideal theranostic nanoplatforms, and a few selected examples are listed in Table 9.

Bian *et al.* constructed a multifunctional MOF with ZIF-8 with gold nanocomposites (AuNCs) and Fe_3O_4@polyacrylic acid (PAA) that was employed to achieve trimodal diagnosis based on MR, CT, and fluorescence, and simultaneous delivery of doxorubicin (DOX) to the targeted tissue. Confocal laser scanning microscopy (CLSM) images showed 2.5 times higher fluorescence intensity of the MOF system, compared to the discrete gold nanocomposites. *In vitro* studies of HepG-2 cells for 24 h at 37 °C under 5% CO_2 displayed strong orange fluorescence from the cytoplasm of the cells, which validated efficient uptake by the cell lines. As the concentration of MOFs rises, Hounsfield units (HU) for CT imaging are continuously increased too, proving that the MOF was ideal for CT. The structure showed an attenuation effect with concentration, indicating its potential as a T2 contrast agent in MRI. Further, the MOF was found to be highly efficient for pH-stimulated drug delivery, with 81% drug loading capacity and 68% drug delivery rate after 26 hours at pH 5.3.[64,65]

The use of nanoparticles has been also reported by Guo and co-workers wherein they used core–shell gold nanorods and mesoporous silica to synthesize a Fe-based MOF with

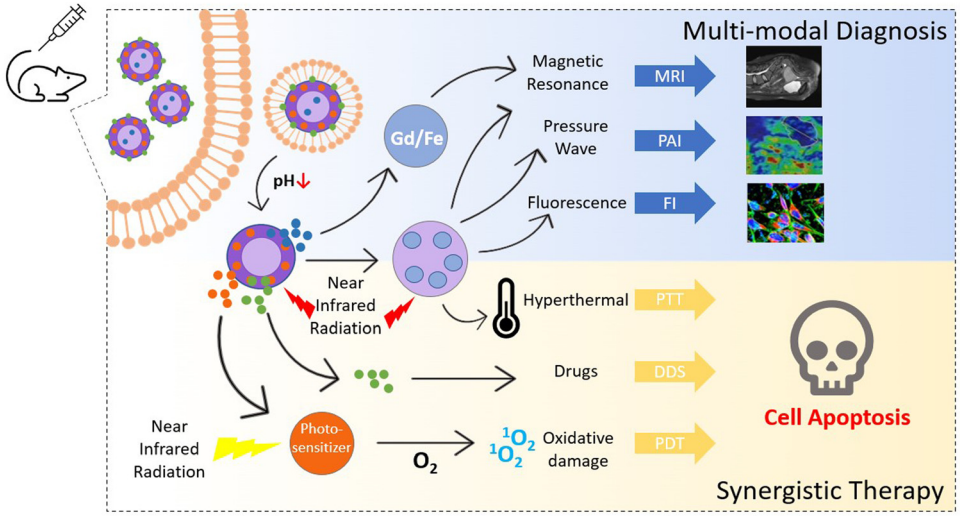

Fig. 12 Illustrative depiction of applications of MOFs in multimodal theranostic procedures encompassing magnetic resonance imaging (MRI), photoacoustic imaging (PAI), fluorescence imaging (FI), photothermal therapy (PTT), drug delivery system (DDS), and photodynamic therapy (PDT). Adapted from ref. 66 with permission from the Royal Society of Chemistry, copyright 2021.

Table 9 Multimodal imaging-guided synergistic treatment *via* MOFs

Entry	MOF used	Target cell lines	Drug delivered	Imaging modality	Therapeutic strategies	Findings	Ref.
1	Fe_3O_4@PAA/AuNCs/ZIF-8	HepG2	Doxorubicin (DOX)	MRI, CT, FI	Chemotherapy	The MOF exhibited superparamagnetic characteristics, showed an attenuation effect in MRI, demonstrated a linear relationship with the concentration in CT imaging, and high-intensity fluorescence in CLSM images was observed. DOX loading capacity was found to be 81% and drug release was 68% at pH 5.3 after 26 hours	64
2	DOX@GNRs-MSNs-MA-MOF	4T1	Doxorubicin (DOX)	MRI, CT, PAI	Chemotherapy, PTT	A high cell mortality rate (85.5%) was seen in combined treatment with chemotherapy and phototherapy. The r1/r2 ratio for T2 contrast in MRI was found to be 9.8. Strong CT and PAI signals were observed in the tumor regions of mice	65
3	Gd–PDA Ce6@Gd-MOF	4T1	—	MRI, PAI	PDT, PTT	Cell apoptosis in PTT/PDT combination was higher than in PTT or PDT alone. Gd ions were found to be efficient in MRI. Strong absorption in 880 nm NIR radiation, positive correlation with nanoparticle concentration, and strong signaling at tumor sites demonstrated great potential in PAI	66

hyaluronic acid and DOX as the loaded drug. The hyaluronic acid-treated MOF displayed stronger red fluorescence in 4T1 breast cancer cells, indicating its well-targeted cellular uptake. The combined photothermal thermal therapy with chemotherapy enhanced the cell mortality rate which reached up to 85.5%. Along with its therapeutic efficiency, favorable imaging capabilities were also seen in the MOF. *In vivo* imaging studies revealed gradual darkening of MR images with the increase in Fe concentration and the r1/r2 ratio was found to be 9.8, proving the ability of the MOF as a superb T2 contrast agent in MRI. Moreover, through intravenous injection of the MOF in the mice's body, well-targeted strong signals in localized tumor cells were displayed in CT and PA imaging which increased as the MOF concentration increased.[65]

Interestingly, synergistic treatment with PDT and PTT has been linked to better results in killing cancer cells and it circumvents the limitations of individual therapeutic techniques. The hyperthermal effect of PTT and oxidative damage to cancer cells by PDT complement each other and lead to stronger tissue penetration and increased cell death. A gadolinium (Gd) ion-doped MOF, incorporated with polydopamine (PDA) nanoparticles and Ce6 as a photosensitizer, was formulated by Pu *et al.* for achieving PTT/PDT synergistic treatment along with multimodal imaging. The PTT/PDT combination led to a higher cell apoptosis rate (over 74%) and increased cytotoxicity in cancer cells, which was more than the achievable rates through individual treatments. Moreover, *in vivo* and *in vitro* imaging analysis confirmed the great efficiency of the MOF as a T2 contrast agent in MRI and as a prospective nanoplatform for photoacoustic signaling.[66]

6. Biocompatibility and pharmacokinetics

Even if drugs are effective, they should be compatible with the human body in such a way that they don't cause harm to the

patient. If the body accepts the drug, it means it is biocompatible, otherwise it can cause an immunological response and could become toxic. This is determined by various factors including the organic linker, the nature of the metal, and even the physical properties of the MOF. Toxicity is measured using some key factors like degradation kinetics, biodistribution, accumulation in the body, absorption in the blood, and excretion.

Since cancer cells are slightly acidic and ZIF is compatible with the normal pH of the body, the drug release is very low for healthy cells with a pH of 7.4 and the drug is released at acidic pH by dissociation.[61] Cytotoxic effects are not seen in the body as it is stable at neutral pH. Similarly, Fe-MIL-101 displayed selective cytotoxicity due to the differences in the ability to select between the cancer cells and normal cells. In the test, selective toxicity is seen against HeLa, A549, and SKOV3 cancer cells and HUVEC cells but lower toxicity is observed towards normal BABL-3T3 cells. Fe-MIL-101 showed cytotoxicity, depending on the time of administration, towards almost all cells except HeLa and BABL-3T3 cells. The concentration present in the treatment after 72 hours showed high variability compared to 24 and 48 hours, thus revealing the biodegradability of Fe-MIL-101.[52] Regarding treatment with Mn-MOF, even though it was directly injected into the tumor, it showed very little effect on other organs thus affirming its low *in vivo* cytotoxicity. All the test groups also showed very little or no body weight change in mice after 14 days of treatment, thus showing the time independent effect of the medicine.

In chemotherapy, treatment with sMoSe2-ICG NSs did not show any significant difference in the body weight of the mice. Even though this indicated the non-toxicity of the MOF, it should be noted that the nanosheets of this MOF would be excreted by the body completely within 36 hours, according to photoacoustic imaging, showing great biodegradability. It further revealed that sMoSe2-ICG NSs did not affect the function of blood and showed great histocompatibility. Toxicity studies revealed that sMoSe2-ICG NSs display very little cytotoxicity which leads to lower *in vivo* toxicity.[56] UMOF-TiO_2 showed both Type I and II ROS production PDTs. In addition, no biological damage wasdiscernible by the MTT assay which was exerted by the MOF to the cells even after being incubated with MCF-7 for a day with concentrations as high as 200 μg mL^{-1}. This indicated that UMOF-TiO_2 is highly biocompatible. Histopathological evaluation by hematoxylin and eosin (H&E) staining did not find organ damage in mice and recorded normal healthy weight in them upon the administration of porphyrin palladium MOFs for photoacoustic imaging and hydrogenothermal cancer therapy.[59]

In SDT, the performance of DHMS was assessed. Cytotoxicity was not observed at a high concentration of 100 μg mL^{-1} following the incubation time of 24 hours.[63] Another MOF used in SDT has been TiO_2/C; to assess its biosafety, a hemolysis assay was conducted using a murine model. The results showed the rate of hemolysis of all samples tested to be lower than 5%. Then, healthy mice were intravenously injected and they did not show any decrease in body weight for 14 days after treatment. On the 14th day after treatment, histopathological analysis of the major tissues showed no inflammation or damage, thus revealing its superior biocompatibility and its potential for *in vivo* treatment.[62]

In addition to biocompatibility, the pharmacokinetics of MOFs is a very relevant and important topic of discussion. Kush *et al.* researched the efficacy of gemcitabine (GEM) by using the MOF MIL-100 as a capsule to transport GEM. The pharmacokinetic test entailed intravenous injection of GEM and MIL 100-GEM by randomly dividing the male Wistar rats deployed into 2 groups. One group was injected with GEM and the other with MIL 100-GEM with a dose of 40 mg kg^{-1}.[67] Another experiment was performed by Ahmadi *et al.* to understand the pharmacokinetics of ZIF-8 nMOF treated with technetium-99m [^{99m}Tc]. Here, they injected 1000 μCi pertechnate in the control group and the second group was injected with [^{99m}Tc]-ZIF-8 NPs. Both the groups had six rats and the blood sample was collected in 8 different intervals.[68]

Multiple parameters affect the pharmacokinetics which include properties and characteristics like the surface, size of the particle, the rigidity of the particle, *etc.* The PK quantification by Kush *et al.* was accomplished by HPLC (high performance liquid chromatography) and it was found that the administration of MIL100-GEM showcased comparatively slow removal from the circulatory system. It was understood that the PK of MIL100-GEM was at least 16 times the intensive pharmacokinetics of GEM alone.[67]

The PK studies by Ahmadi *et al.*, similar to the above experiment, revealed that the control group had lost most of pertechnate from the system while the ones injected with [^{99m}Tc]-ZIF-8 NPs exhibited a rapid decrease in its level in the blood in the beginning hour of the experiment. However, the removal of [^{99m}Tc]-ZIF-8 was slowed down over the next 24 hours.[68]

7. Conclusion and future prospects

With the advancements in technology and research, modern medicine can expand its boundaries in developing innovative techniques for detecting and curing diseases that were once deemed incurable. Metal–organic frameworks (MOFs) provide enlightening opportunities in diverse multifaceted aspects of cancer research that can offer efficient alternatives to conventional techniques for cancer detection and treatment. Their remarkable potential for biosensing and cancer imaging strengthens modern-day diagnosis. Various paramagnetic or superparamagnetic cores in conjugation with a diverse range of nanoparticles deliver strong signaling, clear visualization, high tissue penetration, and stability, and overall provide fast and precise imaging of tumors, thus enhancing the existing techniques by many folds. Detection of cancer at the earliest has also been made possible through MOFs due to their ability to detect cancer biomarkers at even strikingly low concentrations. This manifests the paramount significance of MOFs in the world of detection and diagnosis.

The excellent features of MOFs find vivid applications for therapeutic strategies, opening new dimensions in cancer treatment. Site-specific delivery of a variety of natural and artificial agents, anticancer drugs, and nanoparticles, and well-targeted working principles of MOFs in advanced cancer

therapies like starvation therapy, gene therapy, photothermal therapy, photodynamic therapy, *etc.*, crucially eliminate side effects and could lead to higher effectiveness in treatment, giving them an edge over the traditional procedures. Further, the integration of compatible therapeutic and diagnostic techniques through MOFs for administering synergistic combination therapies and multimodal theranostics is a holistic approach toward attaining cumulative benefits and compensating for the limitations of individual strategies.

But, even after all the research advancements and extremely promising results displayed by MOFs in numerous anti-cancer studies, clinical trials have not been started yet. Currently, the studies are strictly limited to *in vivo* mouse models. The actual capability of such novel approaches still remains hazy unless they are tried on humans. In order to achieve this, further studies on the biocompatibility and cytotoxicity of MOFs ought to be performed. Also, concrete safety guarantees and scientific protocols would have to be designed for the purpose. While most of the research on MOFs is focused on the outcomes, much effort must be devoted to understanding the metabolic mechanisms behind these results. Long-term monitoring of the accumulation of nanoparticles in the body, interaction with tissue microenvironments, and circulation through the bloodstream needs to be addressed. In the coming years, more research would emerge on applications of MOFs in cancer diagnosis and treatment, which would enable us to detect cancer at the earliest, find a permanent cure, and cut down the side effects to a large extent. MOFs remain the bright horizon in the path of medical research that would be certainly reachable in the coming years.

Abbreviations

4-ATP	4-Aminothiophenol
AFP	Alpha-fetoprotein
AIAs	Angiogenesis inhibiting agents
ART	Artemisinin
BA	Boswellic acid
BDC	Benzene-1,3,5-tricarboxylic acid
BSA	Bovine serum albumin
BTC	1,3,5-Benzenetricarboxylate
CA125	Carbohydrate antigen 125
CCM	Curcumin
CLSM	Confocal laser scanning microscopy
CPT	Camptothecin
CS	Chitosan
CT	Computed tomography
DBP	5,15-Di(*p*-benzoato)porphyrin
DDS	Drug delivery system
DHA	Dihydroartemisinin
DHMS	Double-layer hollow manganese silicate nanoparticle
DMF	Dimethylformamide
DOX	Doxorubicin
DS	Diclofenac sodium
FI	Fluorescence imaging
FRET	Fluorescence resonance energy transfer
GEM	Gemcitabine
H&E	Hematoxylin and eosin
H_3BCB	Benzenetricarbonyltribenzoic acid
HPLC	High performance liquid chromatography
HU	Hounsfield units
ISC	Intersystem crossing
MDM2	Murine double minute 2
MIL	Materials of Institut Lavoisier
MOFs	Metal–organic frameworks
MRI	Magnetic resonance imaging
MTX	Methotrexate
NIM	Nimesulide
NIR	Near-infrared
NMOF	Nanoscale metal–organic framework
NPs	Nanoparticles
NSAIDs	Non-steroidal anti-inflammatory drugs
PAA	Polyacrylic acid
PAI	Photoacoustic imaging
PCP	Porous coordination polymers
PDA	Polydopamine
PDT	Photodynamic therapy
PK	Pharmacokinetics
PL	Photoluminescence
PNIPAM	Thermoresponsive polymer
PS	Photosensitizer
PTT	Photothermal therapy
PTX	Paclitaxel
ROS	Reactive oxygen species
SAV	Surface accessible volume
SDT	Sonodynamic therapy
SERS	Surface enhanced Raman scattering
SOSG	Singlet oxygen sensor green
TACE	Transarterial chemoembolization
TCPP	Tetra(4-carboxyphenyl)porphine
UCNPs	Upconversion nanoparticles
US	Ultrasound
XRD	X-ray diffraction
α-CHC	α-Cyano-4-hydroxycinnamic acid

Conflicts of interest

The authors declare no conflict of interest, financial or otherwise.

References

1 Editorial, The global challenge of cancer, *Nat Cancer*, 2020, **1**, 1–2.
2 S. L. James, *Chem. Soc. Rev.*, 2003, **32**, 276–288.
3 Z. C. Kampouraki, D. A. Giannakoudakis, V. Nair, A. Hosseini-Bandegharaei, J. C. Colmenares and E. A. Deliyanni, *Molecules*, 2019, **24**, 4525.
4 M. R. Saeb, N. Rabiee, M. Mozafari, F. Verpoort, L. G. Voskressensky and R. Luque, *Materials*, 2021, **14**, 7277.

5 S. Keskin and S. Kizilel, *Ind. Eng. Chem. Res.*, 2011, **50**, 1799–1812.
6 D. Zhao, W. Zhang, S. Yu, S. L. Xia, Y. N. Liu and G. J. Yang, *J. Nanobiotechnol.*, 2022, **20**, 421.
7 X. Huang, X. Sun, W. Wang, Q. Shen, Q. Shen, X. Tang and J. Shao, *J. Mater. Chem. B*, 2021, **9**, 3756–3777.
8 G. Lan, K. Ni and W. Lin, *Coord. Chem. Rev.*, 2019, **379**, 65–81.
9 S. Gulati, P. Singh, A. Diwan, A. Mongia and S. Kumar, *RSC Med. Chem.*, 2020, **11**, 1252–1266.
10 S. Gulati, N. Mansi, S. Vijayan, S. Kumar, V. Agarwal, B. Harikumar and R. S. Varma, *Mater. Adv.*, 2022, **3**, 2971–2989.
11 S. Kumar, A. Mongia, S. Gulati, P. Singh, A. Diwan and S. Shukla, *Cancer Treat. Res. Commun.*, 2020, **25**, 100258.
12 S. Kumar, A. Diwan, P. Singh, S. Gulati, D. Choudhary, A. Mongia, S. Shukla and A. Gupta, *RSC Adv.*, 2019, **9**, 23894–23907.
13 J. Yang and Y. W. Yang, *Small*, 2020, **16**, 1906846.
14 M. X. Wu and Y. W. Yang, *Adv. Mater.*, 2017, **29**, 1606134.
15 Y. Wang, J. Yan, N. Wen, H. Xiong, S. Cai, Q. He, Y. Hu, D. Peng, Z. Liu and Y. Liu, *Biomaterials*, 2020, 230.
16 D. Zhao, D. J. Timmons, D. Yuan and H. C. Zhou, *Acc. Chem. Res.*, 2011, **44**, 123–133.
17 R. J. Kuppler, D. J. Timmons, Q. R. Fang, J. R. Li, T. A. Makal, M. D. Young, D. Yuan, D. Zhao, W. Zhuang and H. C. Zhou, *Coord. Chem. Rev.*, 2009, **253**, 3042–3066.
18 Y. Pan, Y. Liu, G. Zeng, L. Zhao and Z. Lai, *Chem. Commun.*, 2011, **47**, 2071–2073.
19 Y. K. Seo, J. W. Yoon, J. S. Lee, U. H. Lee, Y. K. Hwang, C. H. Jun, P. Horcajada, C. Serre and J. S. Chang, *Microporous Mesoporous Mater.*, 2012, **157**, 137–145.
20 W. J. Son, J. Kim, J. Kim and W. S. Ahn, *Chem. Commun.*, 2008, 6336–6338.
21 J. Beamish-Cook, K. Shankland, C. A. Murray and P. Vaqueiro, *Cryst. Growth Des.*, 2021, **21**, 3047–3055.
22 S. Feng, X. Zhang, D. Shi and Z. Wang, *Front. Chem. Sci. Eng.*, 2021, **15**, 221–237.
23 M. Özsoy, V. Atiroğlu, G. Guney Eskiler, A. Atiroğlu, A. Deveci Ozkan and M. Özacar, *Colloids Surf., B*, 2021, **204**, 111788.
24 F. Jeremias, S. K. Henninger and C. Janiak, *Dalton Trans.*, 2016, **45**, 8637–8644.
25 P. Horcajada, H. Chevreau, D. Heurtaux, F. Benyettou, F. Salles, T. Devic, A. Garcia-Marquez, C. Yu, H. Lavrard, C. L. Dutson, E. Magnier, G. Maurin, E. Elkaïm and C. Serre, *Chem. Commun.*, 2014, **50**, 6872–6874.
26 P. Horcajada, S. Surblé, C. Serre, D. Y. Hong, Y. K. Seo, J. S. Chang, J. M. Grenèche, I. Margiolaki and G. Férey, *Chem. Commun.*, 2007, 2820–2822.
27 Y. Gossuin, A. Hocq, P. Gillis and V. Quoc Lam, *J. Phys. D: Appl. Phys.*, 2010, 43.
28 S. M. Sheta, S. M. El-Sheikh, M. M. Abd-Elzaher, S. R. Salem, H. A. Moussa, R. M. Mohamed and I. A. Mkhalid, *Appl. Organomet. Chem.*, 2019, **33**, e5249.
29 M. Wang, M. Hu, Z. Li, L. He, Y. Song, Q. Jia, Z. Zhang and M. Du, *Biosens. Bioelectron.*, 2019, **142**, 111536.
30 X. Qiao, B. Su, C. Liu, Q. Song, D. Luo, G. Mo and T. Wang, *Adv. Mater.*, 2018, **30**, 1702275.
31 A. Afzalinia and M. Mirzaee, *ACS Appl. Mater. Interfaces*, 2020, **12**, 16076–16087.
32 W. A. Kalender, *Phys. Med. Biol.*, 2006, **51**, R29.
33 K. E. Dekrafft, Z. Xie, G. Cao, S. Tran, M. Liqing, O. Z. Zhou and W. Lin, *Angew. Chem., Int. Ed.*, 2009, **48**, 9901–9904.
34 H. Alijani, A. Noori, N. Faridi, S. Z. Bathaie and M. F. Mousavi, *J. Solid State Chem.*, 2020, **292**, 121680.
35 S. Hindocha, *Johnson Matthey Technology Review*, Johnson Matthey Public Limited Company, 2017, vol. 61, pp. 138–141.
36 W. Lin, Q. Hu, J. Yu, K. Jiang, Y. Yang, S. Xiang, Y. Cui, Y. Yang, Z. Wang and G. Qian, *ChemPlusChem*, 2016, **81**, 804–810.
37 R. Abazari, A. R. Mahjoub, F. Ataei, A. Morsali, C. L. Carpenter-Warren, K. Mehdizadeh and A. M. Z. Slawin, *Inorg. Chem.*, 2018, **57**, 13364–13379.
38 H. Chen, B. Sun, S. Pan, H. Jiang and X. Sun, *Anticancer Drugs*, 2009, **20**, 131–140.
39 Y. Li, Y. Song, W. Zhang, J. Xu, J. Hou, X. Feng and W. Zhu, *J. Mater. Chem. B*, 2020, **8**, 7382–7389.
40 W. Du, C. Pang, Y. Xue, Q. Zhang and X. Wei, *Oncol. Lett.*, 2015, **10**, 3266–3270.
41 E. Naderali, B. Valipour, A. A. Khaki, J. S. Rad, A. Alihemmati, M. Rahmati and H. N. Charoudeh, *Adv. Pharm. Bull.*, 2019, **9**, 470–480.
42 Y. Xiao, D. Liu, C. Liu, Y. Wang and C. Wang, *J. Solid State Chem.*, 2020, **292**, 121685.
43 B. Singh, P. G. Reddy, A. Goberdhan, C. Walsh, S. Dao, I. Ngai, T. C. Chou, P. O-charoenrat, A. J. Levine, P. H. Rao and A. Stoffel, *Genes Dev.*, 2002, **16**, 984–993.
44 L. L. Sun, Y. H. Li and H. Shi, *J. Cluster Sci.*, 2019, **30**, 251–258.
45 K. Sethi, S. Sharma and I. Roy, *RSC Adv.*, 2016, **6**, 76861–76866.
46 F. Ke, Y. P. Yuan, L. G. Qiu, Y. H. Shen, A. J. Xie, J. F. Zhu, X. Y. Tian and L. De Zhang, *J. Mater. Chem.*, 2011, **21**, 3843–3848.
47 Y. N. Wu, M. Zhou, S. Li, Z. Li, J. Li, B. Wu, G. Li, F. Li and X. Guan, *Small*, 2014, **10**, 2927–2936.
48 K. Jiang, L. Zhang, Q. Hu, Q. Zhang, W. Lin, Y. Cui, Y. Yang and G. Qian, *Chem. – Eur. J.*, 2017, **23**, 10215–10221.
49 M. H. Teplensky, M. Fantham, P. Li, T. C. Wang, J. P. Mehta, L. J. Young, P. Z. Moghadam, J. T. Hupp, O. K. Farha, C. F. Kaminski and D. Fairen-Jimenez, *J. Am. Chem. Soc.*, 2017, **139**, 7522–7532.
50 D. Wang, J. Zhou, R. Shi, H. Wu, R. Chen, B. Duan, G. Xia, P. Xu, H. Wang, S. Zhou, C. Wang, H. Wang, Z. Guo and Q. Chen, *Theranostics*, 2017, **7**, 4605–4617.
51 D. Wang, J. Zhou, R. Chen, R. Shi, G. Zhao, G. Xia, R. Li, Z. Liu, J. Tian, H. Wang, Z. Guo, H. Wang and Q. Chen, *Biomaterials*, 2016, **100**, 27–40.
52 J. Wang, D. Chen, B. Li, J. He, D. Duan, D. Shao and M. Nie, *Sci. Rep.*, 2016, **6**, 26126.
53 X. Leng, X. Dong, W. Wang, N. Sai, C. Yang, L. You, H. Huang, X. Yin and J. Ni, *Molecules*, 2018, **23**, 2490.
54 Y. Li, G. Liu, J. Ma, J. Lin, H. Lin, G. Su, D. Chen, S. Ye, X. Chen, X. Zhu and Z. Hou, *J. Controlled Release*, 2017, **258**, 95–107.
55 Z. Liu, T. Li, F. Han, Y. Wang, Y. Gan, J. Shi, T. Wang, M. L. Akhtar and Y. Li, *Biomater. Sci.*, 2019, **7**, 3683–3692.

56 J. Chen, X. Li, X. Liu, H. Yan, Z. Xie, Z. Sheng, X. Gong, L. Wang, X. Liu, P. Zhang, H. Zheng, L. Song and C. Liu, *Biomater. Sci.*, 2018, **6**, 1503–1516.
57 Y. Liu, P. Bhattarai, Z. Dai and X. Chen, *Chem. Soc. Rev.*, 2019, **48**, 2053–2108.
58 K. Lu, C. He and W. Lin, *J. Am. Chem. Soc.*, 2015, **137**, 7600–7603.
59 Z. Shi, K. Zhang, S. Zada, C. Zhang, X. Meng, Z. Yang and H. Dong, *ACS Appl. Mater. Interfaces*, 2020, **12**, 12600–12608.
60 J. Lu, L. Yang, W. Zhang, P. Li, X. Gao, W. Zhang, H. Wang and B. Tang, *Chem. Commun.*, 2019, **55**, 10792–10795.
61 L. Rengeng, Z. Qianyu, L. Yuehong, P. Zhongzhong and L. Libo, *Photodiagn. Photodyn. Ther.*, 2017, **19**, 159–166.
62 J. Cao, Y. Sun, C. Zhang, X. Wang, Y. Zeng, T. Zhang and P. Huang, *Acta Biomater.*, 2021, **129**, 269–279.
63 X. Pan, W. Wang, Z. Huang, S. Liu, J. Guo, F. Zhang, H. Yuan, X. Li, F. Liu and H. Liu, *Angew. Chem., Int. Ed.*, 2020, **59**, 13557–13561.
64 R. Bian, T. Wang, L. Zhang, L. Li and C. Wang, *Biomater. Sci.*, 2015, **3**, 1270–1278.
65 H. Guo, S. Yi, K. Feng, Y. Xia, X. Qu, F. Wan, L. Chen and C. Zhang, *Chem. Eng. J.*, 2021, **403**, 126432.
66 Y. Pu, Y. Zhu, Z. Qiao, N. Xin, S. Chen, J. Sun, R. Jin, Y. Nie and H. Fan, *J. Mater. Chem. B*, 2021, **9**, 1846–1857.
67 P. Kush, T. Bajaj, M. Kaur, J. Madan, U. K. Jain, P. Kumar, A. Deep and K. H. Kim, *J. Inorg. Organomet. Polym. Mater.*, 2020, **30**, 2827–2841.
68 M. Ahmadi, M. Khoramjouy, S. Dadashzadeh, E. Asadian, M. Mosayebnia, P. Geramifar, S. Shahhosseini and F. Ghorbani-Bidkorpeh, *J. Drug Delivery Sci. Technol.*, 2023, **81**, 104249.